

## ORIGINAL RESEARCH

## Toll-like Receptor 9 Promotes Initiation of Gastric Tumorigenesis by Augmenting Inflammation and Cellular Proliferation



Ke Tang,<sup>1,2</sup> Louise McLeod,<sup>1,2</sup> Thaleia Livis,<sup>1,2</sup> Alison C. West,<sup>1,2</sup> Ruby Dawson,<sup>1,2</sup> Liang Yu,<sup>1,2</sup> Jesse J. Balic,<sup>1,2</sup> Michelle Chonwerawong,<sup>1,2</sup> Georgie Wray-McCann,<sup>1,2</sup> Hiroko Oshima,<sup>3</sup> Masanobu Oshima,<sup>3</sup> Virginie Deswaerte,<sup>1,2</sup> Richard L. Ferrero,<sup>1,2,4</sup> and Brendan J. Jenkins<sup>1,2</sup>

<sup>1</sup>Centre for Innate Immunity and Infectious Diseases, Hudson Institute of Medical Research, Clayton, Victoria, Australia; <sup>2</sup>Department of Molecular Translational Science, Faculty of Medicine, Nursing and Health Sciences, Monash University, Clayton, Victoria, Australia; <sup>3</sup>Division of Genetics, Cancer Research Institute, Kanazawa University, Kanazawa, Japan; and <sup>4</sup>Biomedicine Discovery Institute, Department of Microbiology, Monash University, Clayton, Victoria, Australia

## SUMMARY

We reveal that the innate immune toll-like receptor 9 (TLR9) promotes the initiating stages of gastric carcinogenesis, including that triggered by *Helicobacter pylori* infection. These findings provide in vivo evidence for TLR9 as a candidate therapeutic target in gastric cancer.

**BACKGROUND & AIMS:** Gastric cancer (GC) is strongly linked with chronic gastritis after *Helicobacter pylori* infection. Toll-like receptors (TLRs) are key innate immune pathogenic sensors that mediate chronic inflammatory and oncogenic responses. Here, we investigated the role of TLR9 in the pathogenesis of GC, including *Helicobacter* infection.

**METHODS:** *TLR9* gene expression was profiled in gastric tissues from GC and gastritis patients and from the spontaneous *gp130<sup>F/F</sup>* GC mouse model and chronic *H felis*-infected wild-type (WT) mice. Gastric pathology was compared in *gp130<sup>F/F</sup>* and *H felis* infection models with or without genetic ablation of *Tlr9*. The impact of *Tlr9* targeting on signaling cascades implicated in inflammation and tumorigenesis (eg, nuclear factor kappa B, extracellular signal-related kinase, and mitogen-activated protein kinase) was assessed in vivo. A direct growth-potentiating effect of TLR9 ligand stimulation on human GC cell lines and *gp130<sup>F/F</sup>* primary gastric epithelial cells was also evaluated.

**RESULTS:** *TLR9* expression was up-regulated in *Helicobacter*-infected gastric tissues from GC and gastritis patients and *gp130<sup>F/F</sup>* and *H felis*-infected WT mice. *Tlr9* ablation suppressed initiation of tumorigenesis in *gp130<sup>F/F</sup>;Tlr9<sup>-/-</sup>* mice by abrogating gastric inflammation and cellular proliferation. *Tlr9<sup>-/-</sup>* mice were also protected against *H felis*-induced gastric inflammation and hyperplasia. The suppressed gastric pathology upon *Tlr9* ablation in both mouse models associated with attenuated nuclear factor kappa B and, to a lesser extent, extracellular signal-related kinase, mitogen-activated protein kinase signaling. TLR9 ligand stimulation of human GC cells and *gp130<sup>F/F</sup>* GECs augmented their proliferation and viability.

**CONCLUSIONS:** Our data reveal that TLR9 promotes the initiating stages of GC and facilitates *Helicobacter*-induced gastric

inflammation and hyperplasia, thus providing in vivo evidence for TLR9 as a candidate therapeutic target in GC. (*Cell Mol Gastroenterol Hepatol* 2022;14:567–586; <https://doi.org/10.1016/j.jcmgh.2022.06.002>)

**Keywords:** Gastric Cancer; Initiation; *H pylori*; TLR9.

Gastric cancer (GC) is the third most lethal cancer worldwide, with 5-year relative survival rates lower than 25% because of the late diagnosis and limited effectiveness of current treatments.<sup>1,2</sup> The major histopathologic type of human GC is intestinal-type adenocarcinoma, which develops stepwise from superficial gastritis (ie, gastric inflammation), atrophic gastritis, intestinal metaplasia, and dysplasia.<sup>3</sup> GC is also divided into cardia and non-cardia topographical subsites in the stomach, the latter of which has a higher frequency and is associated with infection by *Helicobacter pylori*, a Gram-negative bacterial pathogen that accounts for ~6% of the global cancer burden.<sup>4,5</sup>

The strong association between *H pylori*-induced gastritis and GC implicates host immune regulators with pro-tumorigenic activities, albeit currently ill-defined, in promoting the molecular pathogenesis of GC. In this respect, *H pylori* exerts its pathogenicity through interactions with the host mucosal immune system, in which innate immune toll-like receptors (TLRs) play a vital role in recognizing diverse ligands of microbial and host origins to orchestrate the ensuing inflammatory response.<sup>6,7</sup> Over recent years, it has emerged that TLRs may also contribute to the

**Abbreviations used in this paper:** ANOVA, analysis of variance; ERK, extracellular signal-related kinase; GC, gastric cancer; MAPK, mitogen-activated protein kinase; NF-κB, nuclear factor kappa B; PCNA, proliferating cell nuclear antigen; PI3K, phosphatidylinositol-3'-kinase; qPCR, quantitative polymerase chain reaction; TCGA, The Cancer Genome Atlas; TLR, toll-like receptor; TME, tumor microenvironment; WT, wild-type.

Most current article

© 2022 The Authors. Published by Elsevier Inc. on behalf of the AGA Institute. This is an open access article under the CC BY-NC-ND license (<http://creativecommons.org/licenses/by-nc-nd/4.0/>).

2352-345X

<https://doi.org/10.1016/j.jcmgh.2022.06.002>

pathogenesis of human malignancies, including GC, via the regulation of epithelial cell proliferation, apoptosis, epithelial-mesenchymal transition, angiogenesis, metastasis, and immunosuppression through multiple signaling pathways.<sup>4,7-9</sup> These oncogenic TLR-driven responses are transduced via numerous signaling cascades, such as nuclear factor kappa B (NF- $\kappa$ B), extracellular signal-related kinase (ERK) mitogen-activated protein kinase (MAPK), and phosphatidylinositol 3-kinase (PI3K)/Akt.<sup>7,8</sup>

Among TLR family members, clinical studies have shown often contrasting correlations between increased GC risk and single nucleotide polymorphisms in *TLR2*, *TLR4*, *TLR5*, and *TLR9*. This is most likely explained by the high degree of genetic and molecular heterogeneity in human GC, together with study design differences based on patient characteristics (eg, geographical location, ethnicity, age, tumor stage, histologic grade, anatomic location).<sup>4,10</sup> With respect to *TLR2*, its up-regulated expression in tumors from GC patients is associated with poor survival outcomes, and using the *gp130<sup>F/F</sup>* spontaneous mouse model for intestinal-type GC, along with human GC xenografts, we have demonstrated that the up-regulation of *TLR2* in gastric epithelial (tumor) cells promotes tumorigenesis in a tumor cell intrinsic manner (ie, independent of tumor inflammation).<sup>8,11</sup> Despite these observations, a causal role for other TLRs in the molecular pathogenesis of GC remains ill-defined.

*TLR9* is an endosomal sensor of unmethylated CpG-rich DNA motifs and is up-regulated in numerous human cancers affecting the lung, pancreas, breast, esophagus, nasopharynx, and brain, as well as in *H pylori*-positive GC.<sup>4,12-18</sup> Numerous in vitro and in vivo studies have shown that *TLR9* promotes distinct pro-tumorigenic effects in immune and non-immune cells, including angiogenesis, immunosuppression, cell proliferation and invasion.<sup>12-14</sup> Conversely, *TLR9* agonists can also trigger anti-tumor immunity in some cancer types (eg, lung, colon).<sup>19,20</sup> Indeed, the complex and contrasting contribution of *TLR9* signaling to carcinogenesis also extends to gastric inflammation in vivo models induced by *Helicobacter* infection (3-6 weeks), whereby acute host immune responses are either suppressed (neutrophil infiltrates, interferon  $\gamma$  production) or augmented (interleukin 17 production) in infected *Tlr9<sup>-/-</sup>* mice.<sup>21-23</sup>

To provide definitive insights into the mechanistic role of *TLR9* in inflammation-associated GC, here we show that *TLR9* expression was elevated in both uninfected *gp130<sup>F/F</sup>* and chronic (4-month) *Helicobacter*-infected wild-type (WT) mice, as well as in clinical biopsies from GC and *H pylori*-infected gastritis patients. Furthermore, by coupling *Tlr9<sup>-/-</sup>* mice with uninfected *gp130<sup>F/F</sup>* mice, we reveal that the genetic ablation of *Tlr9* suppressed the onset of gastric tumorigenesis, which was accompanied by reduced gastric mucosal inflammation and cellular proliferation. Similarly, *H felis*-induced gastric inflammation and epithelial hyperplasia were ameliorated in *Tlr9<sup>-/-</sup>* mice. Collectively, our findings demonstrate that activation of *TLR9* signaling promotes gastric tumorigenesis in the initiating stage, at

least in part, by augmenting inflammation and cellular proliferation.

## Results

### *TLR9 Expression Is Augmented in Early-Stage Gastric Tumors of Gastric Cancer Patients and Correlates With Impaired Survival*

In 2 independent GC patient cohorts, The Cancer Genome Atlas (TCGA) and an Australian-based mixed Caucasian/Asian cohort, *TLR9* mRNA levels were significantly up-regulated in 78% (14/18) and 65% (13/20) of gastric tumor tissues, respectively, compared with matched adjacent non-tumor tissues (Figure 1A-D, Table 1). Among all TLR family members, only *TLR9* along with *TLR2* were significantly up-regulated in gastric tumor tissues from GC patients; the latter observation for *TLR2* is consistent with our previous report<sup>8,10</sup> (Figure 1A). Interestingly, in the large Gastric Cancer Project '08 - Singapore Patient Cohort comprising tumor only samples (Table 1),<sup>24</sup> the segregation of GC patient primary tumors into either low or high *TLR9* gene expression revealed that high *TLR9* levels were prognostic for impaired overall >10-year survival, with patients expressing high versus low *TLR9* mRNA levels having a median survival of 31.2 versus 56.9 months (Figure 1E). We also note that the stratification of GC patients by disease stage showed that among TLRs, only *TLR9* mRNA expression levels were significantly elevated in early-stage I and II patients compared with advanced-stage III and IV patients (Figure 1F). Collectively, these data indicate that augmented *TLR9* expression is a feature of early-stage human GC.

### *Genetic Targeting of TLR9 in the gp130<sup>F/F</sup> Gastric Cancer Mouse Model Suppresses Tumor Initiation, but not Progression*

We next assessed the expression of *Tlr9* by quantitative polymerase chain reaction (qPCR) in the preclinical *gp130<sup>F/F</sup>* GC mouse model, which from 6 weeks of age onward spontaneously develops antral gastric intestinal-type tumors (with 100% penetrance) that progress in size until a maximal growth is reached at 24-26 weeks of age.<sup>8,25,26</sup> Although gastric *Tlr9* mRNA levels were unchanged in pre-tumorigenic 4-week-old *gp130<sup>F/F</sup>* mice, *Tlr9* gene expression was significantly elevated (2- to 3-fold) at 12 weeks of age in *gp130<sup>F/F</sup>* gastric antral tumors compared with either adjacent non-tumor antral tissue or normal antral tissues of *gp130<sup>+/+</sup>* (WT) mice (Figure 2A). Notably, laser microdissection coupled with qPCR on gastric tissues from tumor-bearing *gp130<sup>F/F</sup>* versus tumor-free WT mice indicated that *Tlr9* mRNA levels were elevated in the epithelium (enriched for *EpCam* gene expression) versus immune cell-containing stroma (enriched for *Ptprc* (CD45) gene expression) within each gastric tissue genotype, with highest *Tlr9* gene expression observed in the *gp130<sup>F/F</sup>* tumor epithelium (Figure 2B). In support of these observations, *Tlr9* mRNA levels were also significantly higher in primary gastric epithelial cells derived from *gp130<sup>F/F</sup>* versus

WT mice (Figure 2C). Conversely, at 24 weeks of age *Tlr9* mRNA levels were significantly elevated (2- to 3-fold) in *gp130<sup>F/F</sup>* non-tumor antral tissue compared with both *gp130<sup>F/F</sup>* gastric antral tumors and WT antral tissues (Figure 2A).

To define whether a causal relationship exists between increased gastric tumoral expression of TLR9 and the pathogenesis of GC, we generated TLR9-deficient *gp130<sup>F/F</sup>* mice (*gp130<sup>F/F</sup>;Tlr9<sup>-/-</sup>*). By 10 weeks of age (early-stage tumorigenesis), the stomachs and gastric tumors of

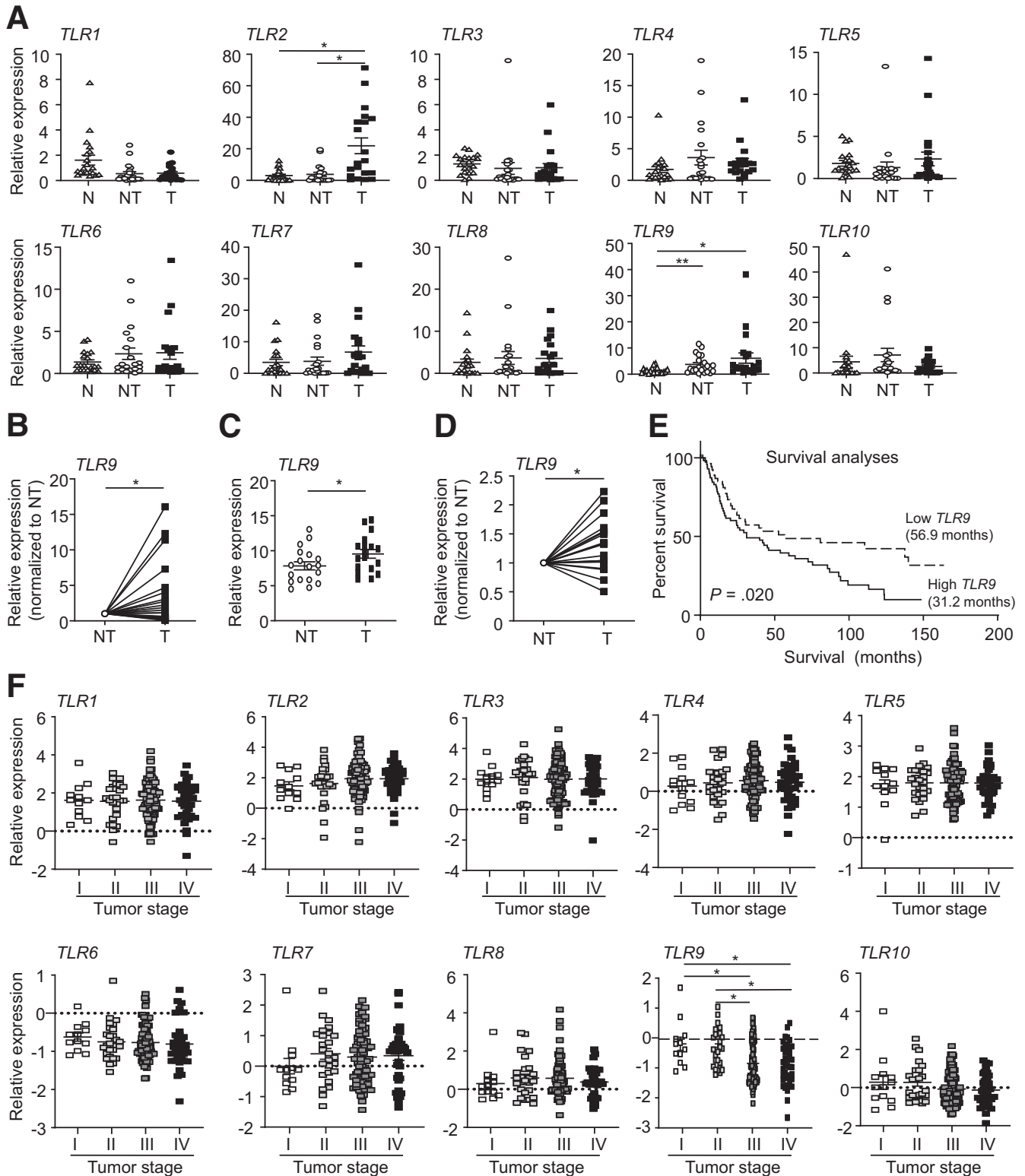


**Table 1.** Clinicopathologic Features and Demographics of the Gastric Cancer Patient Cohorts Used for TLR9 Expression Profiling

	TCGA	Australian	Singapore <sup>a</sup>
Mean age			
Years (range)	66 (50–81)	61.5 (35–84)	68.05 (25–89)
Sex, n (%)			
Male	15 (83.3)	13 (65)	101 (63)
Female	3 (16.7)	7 (35)	50 (31)
Unknown	0 (0)	0 (0)	9 (6)
Histologic type, n (%)			
Intestinal-type	18 (100)	16 (80)	90 (56)
Diffuse	0 (0)	4 (20)	70 (44)
<i>H. pylori</i> status, n (%)			
Positive	1 (5.6)	7 (35)	44 (28)
Negative	4 (22.2)	13 (65)	34 (21)
Unknown	13 (72.2)	0 (0)	82 (51)
Tumor grade, n (%)			
1	2 (11.1)	2 (10)	12 (8)
2	12 (66.7)	8 (40)	27 (17)
3	4 (22.2)	9 (45)	83 (52)
4	0 (0)	1 (5)	38 (23)

TCGA, The Cancer Genome Atlas.

<sup>a</sup>Gastric Cancer Project '08 - Singapore Patient Cohort (GSE15459).

*gp130<sup>F/F</sup>:Tlr9<sup>-/-</sup>* mice were visibly smaller and significantly reduced in weight (49% and 62%, respectively) compared with age-matched *gp130<sup>F/F</sup>* littermates (Figure 2D–F). Surprisingly, however, suppressed gastric tumorigenesis was not apparent in 20-week-old and 30-week-old *gp130<sup>F/F</sup>:Tlr9<sup>-/-</sup>* mice, in which both stomach size and gastric tumor burden were comparable with age-matched *gp130<sup>F/F</sup>* mice (Figure 2G–L). We note that tumor incidence was similar between the genotypes at each age group (Figure 2M). Therefore, genetic ablation of TLR9 in the *gp130<sup>F/F</sup>* GC model preferentially inhibits the early initiation, but not later establishment and progression, stage of gastric tumorigenesis.

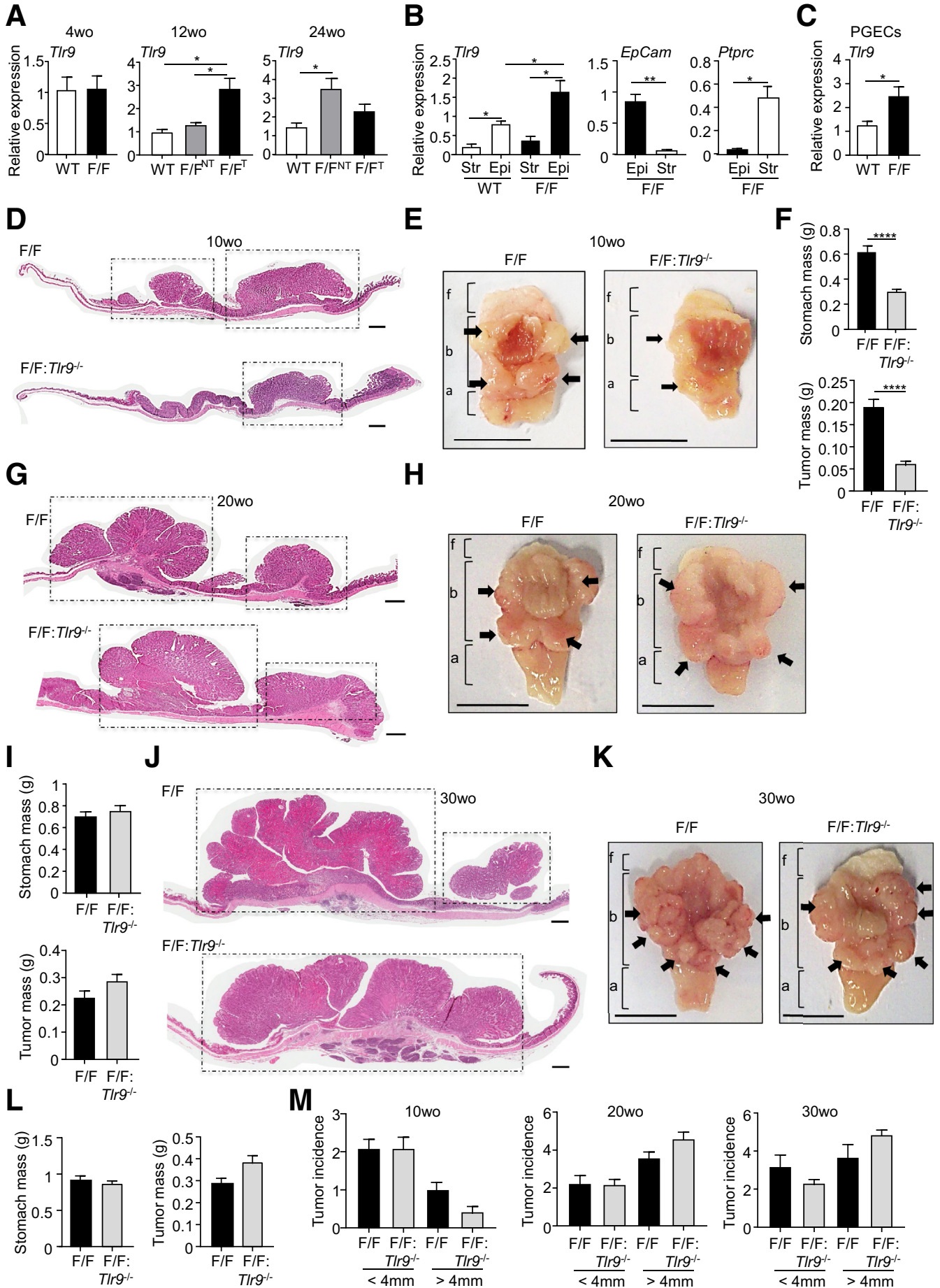
### Suppressed Early-Stage Gastric Tumorigenesis in *gp130<sup>F/F</sup>:Tlr9<sup>-/-</sup>* Mice Is Associated With Reduced Gastric Inflammation and Cellular Proliferation

We next evaluated whether the suppressed early GC phenotype of *gp130<sup>F/F</sup>:Tlr9<sup>-/-</sup>* mice coincided with reduced

tumor-associated inflammation. Indeed, histologic assessment of H&E-stained gastric tissue sections from 10-week-old mice indicated that the inflammation score (chronic inflammatory cell infiltrates in the submucosa and mucosa) in *gp130<sup>F/F</sup>:Tlr9<sup>-/-</sup>* gastric tumors was significantly lower compared with age-matched *gp130<sup>F/F</sup>* tumors (Figure 3A). Immunohistochemical analyses also indicated significantly lower numbers of infiltrating CD45<sup>+</sup> leukocytes, B220<sup>+</sup> B cells, and CD3<sup>+</sup> T cells in the gastric mucosa of 10-week-old *gp130<sup>F/F</sup>:Tlr9<sup>-/-</sup>* versus *gp130<sup>F/F</sup>* mice (Figure 3B–D). The reduced gastric inflammation in smaller *gp130<sup>F/F</sup>:Tlr9<sup>-/-</sup>* tumors was also confirmed at the molecular level, as evidenced by significantly lower mRNA levels of inflammatory genes (*Tnfa*, *Cxcl1*, *Cxcl2*) and protein levels of tumor necrosis factor  $\alpha$  in 10-week-old *gp130<sup>F/F</sup>:Tlr9<sup>-/-</sup>* versus *gp130<sup>F/F</sup>* gastric tumors (Figure 3E and F). By contrast, the expression of several angiogenesis-related genes (*Mmp2*, *Mmp9*, *Vegf*) was comparable in gastric tumors of *gp130<sup>F/F</sup>:Tlr9<sup>-/-</sup>* and *gp130<sup>F/F</sup>* mice, suggesting that TLR9 does not promote angiogenesis in the early establishment stage of gastric tumorigenesis (Figure 3G).

### Figure 1. (See previous page). TLR9 expression is increased in human GC and correlates with poor prognosis.

(A) Scatter plots showing mRNA expression levels of genes encoding TLR family members in gastric tumors (T) and matched, adjacent non-tumor (NT) tissues from an Australian-based mixed Caucasian/Asian patient cohort (n = 20). Normal (N) gastric tissues from GC-free individuals (mixed Caucasian/Asian) are also included (n = 20). \**P* < .05, \*\**P* < .01; one-way analysis of variance (ANOVA). (B) Expression of *TLR9* in gastric tumor tissues normalized to matched non-tumor tissues in the patient cohort from (A). \**P* < .05, paired Student *t* test. (C and D) Expression of *TLR9* in (C) gastric tumors and matched, adjacent non-tumor tissues and (D) gastric tumor tissues normalized to matched non-tumor tissues in TCGA intestinal-type GC patients (n = 18). \**P* < .05; unpaired (C) and paired (D) Student *t* tests. (E) Kaplan-Meier >10-year survival analysis of the Gastric Cancer Project -08 - Singapore Patient Cohort (n = 129) stratified into 2 groups based on low (dashed line) or high (solid line) *TLR9* gene expression. Also shown is the median survival (months). Log-rank (Mantel-Cox) test. (F) Scatter plot showing *TLR9* mRNA expression levels in tumor tissues from intestinal-type GC patients belonging to the Gastric Cancer Project -08 - Singapore Patient Cohort (n = 160) stratified by disease (tumor) stage. \**P* < .05; one-way ANOVA.



Consistent with the comparable gastric tumorigenesis in older (20-week-old)  $gp130^{F/F};Tlr9^{-/-}$  and  $gp130^{F/F}$  mice, similar levels of gastric inflammation were observed in tumors of aged  $gp130^{F/F};Tlr9^{-/-}$  and  $gp130^{F/F}$  mice (Figure 3H–K). We also note a previous report that aberrant activation of M2-type macrophages can be associated with gastric tumor growth in mice.<sup>27</sup> Consistent with this, we observed transcriptional up-regulation of M2-type markers (*Arg1*, *Egr2*), but not M1-type markers (*Cd38*, *Gpr18*), in  $gp130^{F/F}$  gastric tumors (Figure 3L). However, TLR9 deficiency in  $gp130^{F/F};Tlr9^{-/-}$  mice did not alter the gastric expression profile of these M2-type macrophage markers, suggesting TLR9 promotes gastric inflammation and tumorigenesis independent of M2-type macrophage activation (Figure 3L).

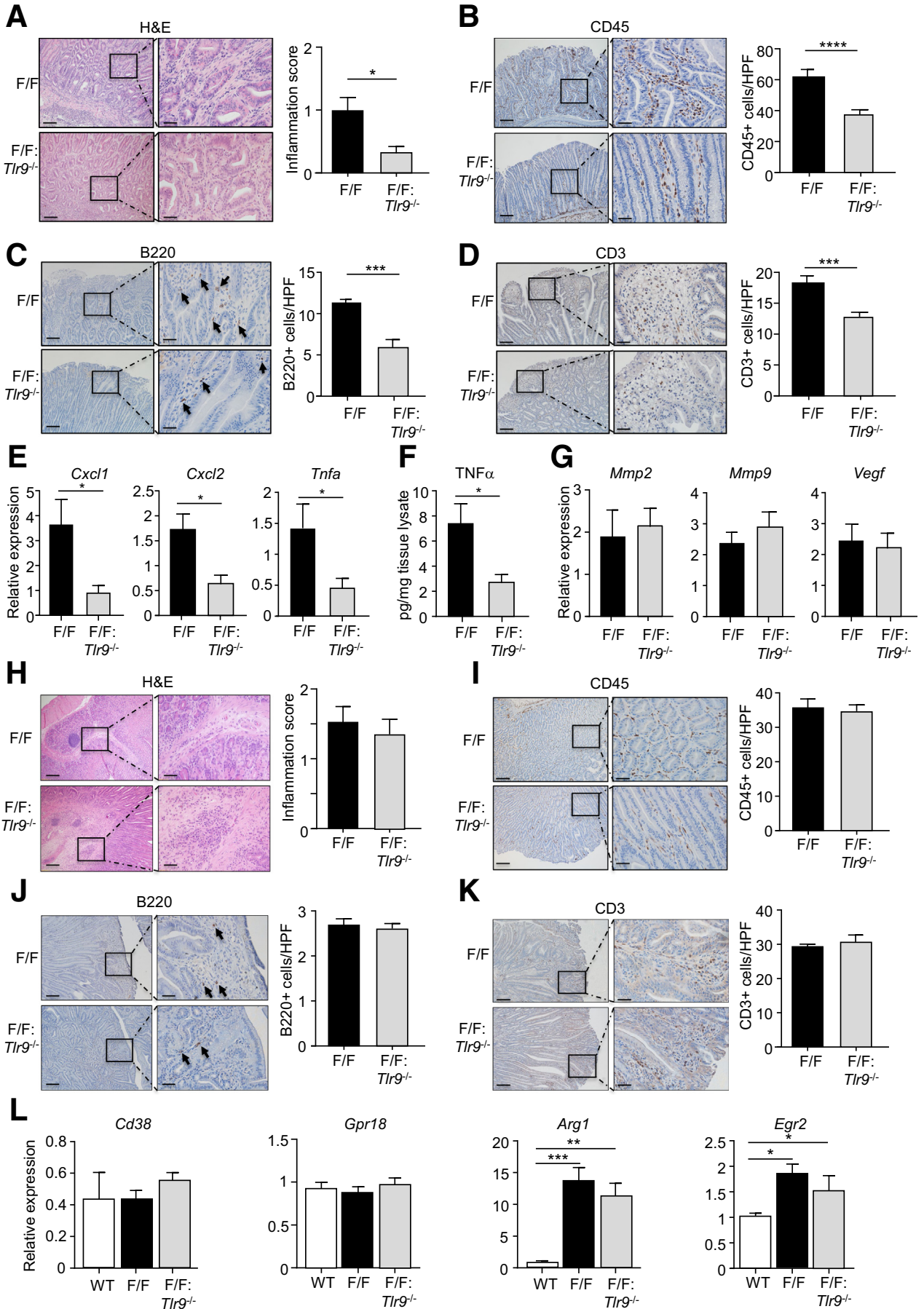
Because elevated gastric epithelial cell proliferation and survival are prominent features of early-stage gastric tumorigenesis in  $gp130^{F/F}$  mice,<sup>8,25</sup> we next investigated whether TLR9 promoted these oncogenic cellular processes in 10-week-old  $gp130^{F/F}$  mice. Indeed, immunohistochemistry indicated that proliferating cell nuclear antigen (PCNA)<sup>+</sup> proliferating cell numbers were significantly decreased (~40%) in the epithelium of gastric tumors of  $gp130^{F/F};Tlr9^{-/-}$  compared with  $gp130^{F/F}$  mice (Figure 4A). These observations were also supported at the molecular level, whereby the expression of a series of proliferative genes (*Bcl2a1*, *Ccnb1*, *Ccnd1*, *Myc*) was significantly reduced in gastric tumors from 10-week-old  $gp130^{F/F};Tlr9^{-/-}$  mice compared with their age-matched  $gp130^{F/F}$  control mice (Figure 4B). By contrast, with respect to cell survival, apoptotic cleaved Caspase-3<sup>+</sup> or TUNEL<sup>+</sup> cell numbers in 10-week-old  $gp130^{F/F};Tlr9^{-/-}$  and  $gp130^{F/F}$  gastric tumors were comparable (Figure 4C and D). Notably, similar levels of cellular proliferation and apoptosis and proliferative gene expression were observed in tumors of aged (20-week-old)  $gp130^{F/F};Tlr9^{-/-}$  and  $gp130^{F/F}$  mice (Figure 4E–G). Collectively, these data indicate that TLR9 selectively promotes cellular proliferation and inflammation during the early

establishment of gastric tumors in the  $gp130^{F/F}$  GC mouse model.

### Suppressed Early-Stage Gastric Tumorigenesis in $gp130^{F/F};Tlr9^{-/-}$ Mice Is Associated With Reduced Activation of Nuclear Factor Kappa B and Extracellular Signal-Related Kinase Mitogen-Activated Protein Kinase Signaling Cascades

To identify TLR9-dependent signaling pathways associated with early-stage gastric tumorigenesis in 10-week-old  $gp130^{F/F}$  mice, we performed Western blots to evaluate the activation (phosphorylation) of NF- $\kappa$ B, ERK1/2 MAPK, PI3K/Akt, and STAT3 pathways. The protein levels of phosphorylated (p) NF- $\kappa$ B p65 and pERK1/2 were significantly lower (42% and 20%, respectively) in gastric tumor lysates of 10-week-old  $gp130^{F/F};Tlr9^{-/-}$  compared with  $gp130^{F/F}$  mice, whereas levels of pAkt and pSTAT3 were comparable between these 2 genotypes (Figure 5A–D). We further verified that reduced tumorigenesis in  $gp130^{F/F};Tlr9^{-/-}$  mice was not a consequence of altered STAT3 signaling, as evidenced by comparable mRNA expression levels of STAT3-target genes (*Socs3*, *I111*) in tumors of 10-week-old  $gp130^{F/F};Tlr9^{-/-}$  and  $gp130^{F/F}$  mice (Figure 5E). Immunohistochemical analyses also confirmed decreased pNF- $\kappa$ B p65<sup>+</sup> and pERK1/2<sup>+</sup> cell numbers in gastric tumors, predominantly the glandular epithelium, of 10-week-old  $gp130^{F/F};Tlr9^{-/-}$  versus  $gp130^{F/F}$  mice, with the reduction again more pronounced for pNF- $\kappa$ B p65 (45%) than pERK1/2 (30%) (Figure 5F and G). By contrast, at 20 weeks of age, expression levels of pNF- $\kappa$ B p65 (very low) and pERK1/2 were comparable in tumors between  $gp130^{F/F};Tlr9^{-/-}$  versus  $gp130^{F/F}$  mice (Figure 5H and I), suggesting that TLR9 does not engage these pathways in later stages of tumorigenesis. Taken together, these data support the notion that genetic targeting of TLR9 inhibits early-stage gastric tumorigenesis in 10-week-old  $gp130^{F/F}$  mice, at least in part, through suppressed activation of NF-

**Figure 2. (See previous page). TLR9 promotes gastric tumorigenesis in 10-week-old  $gp130^{F/F}$  mice.** (A) *Tlr9* expression by qPCR (after normalization for *18S rRNA*) in the indicated gastric antral tissues from 4-week-old, 12-week-old, and 24-week-old  $gp130^{+/+}$  (WT) and  $gp130^{F/F}$  (F/F) mice. NT, non-tumor; T, tumor. n = 6 mice/genotype. \**P* < .05, \*\**P* < .01; unpaired Student *t* tests. (B) qPCR expression analyses of *Tlr9*, *EpCam*, and *Ptprc* (after normalization for *18S rRNA*) in captured laser microdissected gastric epithelial (Epi) and stroma (Str) tissue from WT and/or tumor-bearing F/F mice. n = 4 samples/genotype. \**P* < .05, \*\**P* < .01; one-way ANOVA for *Tlr9*, and paired Student *t* test for *EpCam* and *Prp*. (C) qPCR of *Tlr9* (after normalization for *18S rRNA*) in primary gastric epithelial cells (PGECs) from WT and F/F mice. n = 4 samples/genotype. \**P* < .05; unpaired Student *t* test. (D and E) Representative (D) photomicrographs showing H&E-stained whole scan and (E) macroscopic appearance, of stomachs from 10-week-old F/F and F/F;*Tlr9*<sup>-/-</sup> mice. In (D), tumors are depicted by dotted squares. Scale bars: 1 mm. In (E), arrows indicate macroscopically visible tumors. Fundus (f), body (b), and antral (a) stomach are labeled. Scale bars: 1 cm. (F) Graphs depicting the total mass (g) of stomachs and gastric tumors of 10-week-old F/F and F/F;*Tlr9*<sup>-/-</sup> mice. n = 12 mice/genotype. \*\*\*\**P* < .0001; unpaired Student *t* tests. (G and H) Representative (G) photomicrographs showing H&E-stained whole scans and (H) macroscopic appearance of stomachs from 20-week-old F/F and F/F;*Tlr9*<sup>-/-</sup> mice. In (G), tumors are depicted by dotted squares. Scale bars: 1 mm. In (H), arrows indicate macroscopically visible tumors. Scale bars: 1 cm. (I) Graphs depicting the total mass (g) of stomachs and gastric tumors of 20-week-old F/F and F/F;*Tlr9*<sup>-/-</sup> mice. n = 12 mice/genotype. (J and K) Representative (J) photomicrographs showing H&E-stained whole scans and (K) macroscopic appearance of stomachs from 30-week-old F/F and F/F;*Tlr9*<sup>-/-</sup> mice. In (J), tumors are depicted by dotted squares. Scale bars: 1 mm. In (K), arrows indicate macroscopically visible tumors. Scale bars: 1 cm. (L) Graphs depicting the total mass (g) of stomachs and gastric tumors of 30-week-old F/F and F/F;*Tlr9*<sup>-/-</sup> mice. n = 12 mice/genotype. (M) Graphs depicting total tumor incidence by size in the indicated 10-week-old, 20-week-old, and 30-week-old F/F and F/F;*Tlr9*<sup>-/-</sup> mice. n = 12 mice/genotype.



$\kappa$ B and ERK pathways, but not via PI3K/Akt or STAT3 pathways.

### Increased TLR9 Expression in Human and Mouse Gastric Epithelial (Cancer) Cells Enhances TLR9 Ligand-Driven Cell Growth

Because of the recent emergence that TLR family members (ie, TLR2) can exert pro-tumorigenic effects by directly acting on GC cells to augment their cellular proliferation and survival,<sup>7-9,11</sup> we investigated whether ligand-induced activation of TLR9 could directly enhance the growth responsiveness of human GC cell lines. For this purpose, we used qPCR and Western blotting to stratify a panel of 9 human GC cell lines, along with a control human duodenal cancer cell line (AZ521), into either *TLR9* low-expressing (*TLR9*<sup>Low</sup>) (N87, SNU16, TMK1, AGS, MKN7) and *TLR9* high-expressing (*TLR9*<sup>High</sup>) (SNU601, MKN1, MKN28, NUGC4) cell lines (Figure 6A-C, Table 2). We next stimulated representative *TLR9*<sup>High</sup> NUGC4 and MKN28 cell lines, along with the *TLR9*<sup>Low</sup> AGS cell line as a control, with the TLR9 agonist CpG DNA to measure cell proliferation and cell viability. As shown in Figure 6D and E, both cellular proliferation and viability of *TLR9*<sup>High</sup> NUGC4 and MKN28 cell lines were significantly enhanced on TLR9 ligand stimulation, whereas *TLR9*<sup>Low</sup> AGS cells were non-responsive. The capacity of TLR9 activation to augment the proliferation of gastric (epithelial) cancer cells was also confirmed in TLR9 high-expressing primary gastric epithelial cells from the *gp130*<sup>F/F</sup> GC mouse model, with CpG DNA-stimulated *gp130*<sup>F/F</sup> epithelial cell cultures displaying a significant increase in proliferation compared with control-treated cultures (Figure 6F-H).

Our in vivo data in the *gp130*<sup>F/F</sup> model suggest that TLR9 activates NF- $\kappa$ B and, to a lesser extent, ERK MAPK pathways to promote cellular proliferation within the gastric epithelium during tumorigenesis. To further delineate a role for these pathways in transducing TLR9-induced proliferation and viability of gastric epithelial (cancer) cells, we pretreated NUGC4 and MKN28 human GC cells with well-documented inhibitors of the NF- $\kappa$ B (TPCA-1; I $\kappa$ B kinase-2 inhibitor) and ERK1/2 MAPK (U0126; MAPK kinase inhibitor) pathways before stimulation with

CpG DNA. As shown in Figure 6I, treatment with TPCA-1, but not U0126, resulted in a significant inhibition of TLR9 ligand-stimulated cell proliferation and viability. Taken together, these in vitro data demonstrating enhanced TLR9-driven cellular growth are coincident with our in vivo findings in the *gp130*<sup>F/F</sup> model that TLR9 promotes tumor (epithelial) cell proliferation predominantly via the NF- $\kappa$ B pathway.

### Up-Regulation of TLR9 During *Helicobacter* Infection Exacerbates Gastric Hyperplasia and Inflammation in Vivo

Because *H pylori* infection triggers the initiating pre-neoplastic, chronic gastritis stage of GC,<sup>2,3</sup> we next investigated the pathologic role of TLR9 in *Helicobacter*-induced gastric disease. *TLR9* gene expression profiling of gastric tumors from GC patients stratified for their *H pylori* status revealed that *TLR9* mRNA levels were significantly higher (~1.5- to 2-fold) in *H pylori*-positive patients (TCGA and Australian/Chinese cohorts) compared with the corresponding *H pylori*-negative patients (Figure 7A and B). Similarly, in GC-free individuals, *TLR9* gene expression was elevated (~4-fold) in *H pylori*-positive versus *H pylori*-negative gastric tissues (Figure 7C). Notably, *TLR9* expression in *H pylori*-negative gastric tissues was unchanged irrespective of the grade of gastritis (Figure 7C), suggesting that increased *TLR9* expression in GC-free gastric tissues was specifically associated with *H pylori* infection.

*H felis* strongly colonizes the mouse stomach and induces inflamed, hyperplastic gastric lesions that are similar in pathology to the pre-neoplastic, inflammatory lesions triggered by *H pylori* infection in the human stomach.<sup>28</sup> We therefore established a chronic *H felis* infection model in WT mice, which was characterized by significant increases in stomach weight and gastric corpus mucosal thickness, as well as up-regulation (~3-fold) of *Tlr9* mRNA levels in the gastric body at 4 months after infection, compared with broth control gavaged mice (Figure 7D-G). Notably, *H felis*-infected *Tlr9*<sup>-/-</sup> mice displayed markedly reduced stomach size and weight (32%) and gastric corpus mucosal thickness (25%), compared with *H felis*-infected WT mice (Figure 7E-G). Western blot analyses on gastric tissue lysates from *H felis*

**Figure 3. (See previous page). TLR9 promotes inflammation in tumors of 10-week-old *gp130*<sup>F/F</sup> mice. (A-D)** Representative photomicrographs showing (A) H&E-stained, (B) CD45-stained, (C) B220-stained, and (D) CD3-stained cross sections under low power (left images) and high power (right images) magnification in gastric tumors from 10-week-old (wo) *gp130*<sup>F/F</sup> (F/F) and F/F:*Tlr9*<sup>-/-</sup> mice. Scale bars: 100  $\mu$ m (left images), 25  $\mu$ m (right images). In (A-D), also shown are the corresponding graphs depicting quantification of (A) inflammation scores (0-3; none, mild, moderate, severe) and (B-D) positive cells/high-power field (HPF). n = 6 mice/genotype. \**P* < .05, \*\**P* < .01, \*\*\**P* < .001; unpaired Student *t* tests. (E) qPCR expression of the indicated proinflammatory genes (all relative to 18s rRNA) in gastric tumors from 10wo F/F and F/F:*Tlr9*<sup>-/-</sup> mice. n = 6 mice/genotype. \**P* < .05; unpaired Student *t* test. (F) ELISA for tumor necrosis factor  $\alpha$  in gastric tumor tissues of 10wo F/F and F/F:*Tlr9*<sup>-/-</sup> mice. n = 6 mice/genotype. \**P* < .05; unpaired Student *t* test. (G) qPCR of the indicated angiogenesis genes (all relative to 18s rRNA) in gastric tumors from 10wo F/F and F/F:*Tlr9*<sup>-/-</sup> mice. n = 6 mice/genotype. (H-K) Representative photomicrographs of (H) H&E-stained, (I) CD45-stained, (J) B220-stained, and (K) CD3-stained cross sections under low power (left images) and high power (right images) magnification of gastric tumors from 20wo F/F and F/F:*Tlr9*<sup>-/-</sup> mice. Scale bars: 100  $\mu$ m (left image), 25  $\mu$ m (right image). Also shown are corresponding graphs depicting (H) inflammation scores and (I-K) positive cells/HPF. n = 6 mice/genotype. In (C) and (J), arrows point to representative B220-positive stained cells. (L) qPCR of the indicated M1- and M2-type macrophage marker genes (all relative to 18s rRNA) in gastric tumors from F/F and F/F:*Tlr9*<sup>-/-</sup> mice. n = 6 mice/genotype. \**P* < .05, \*\**P* < .01, \*\*\**P* < .001; one-way ANOVA.

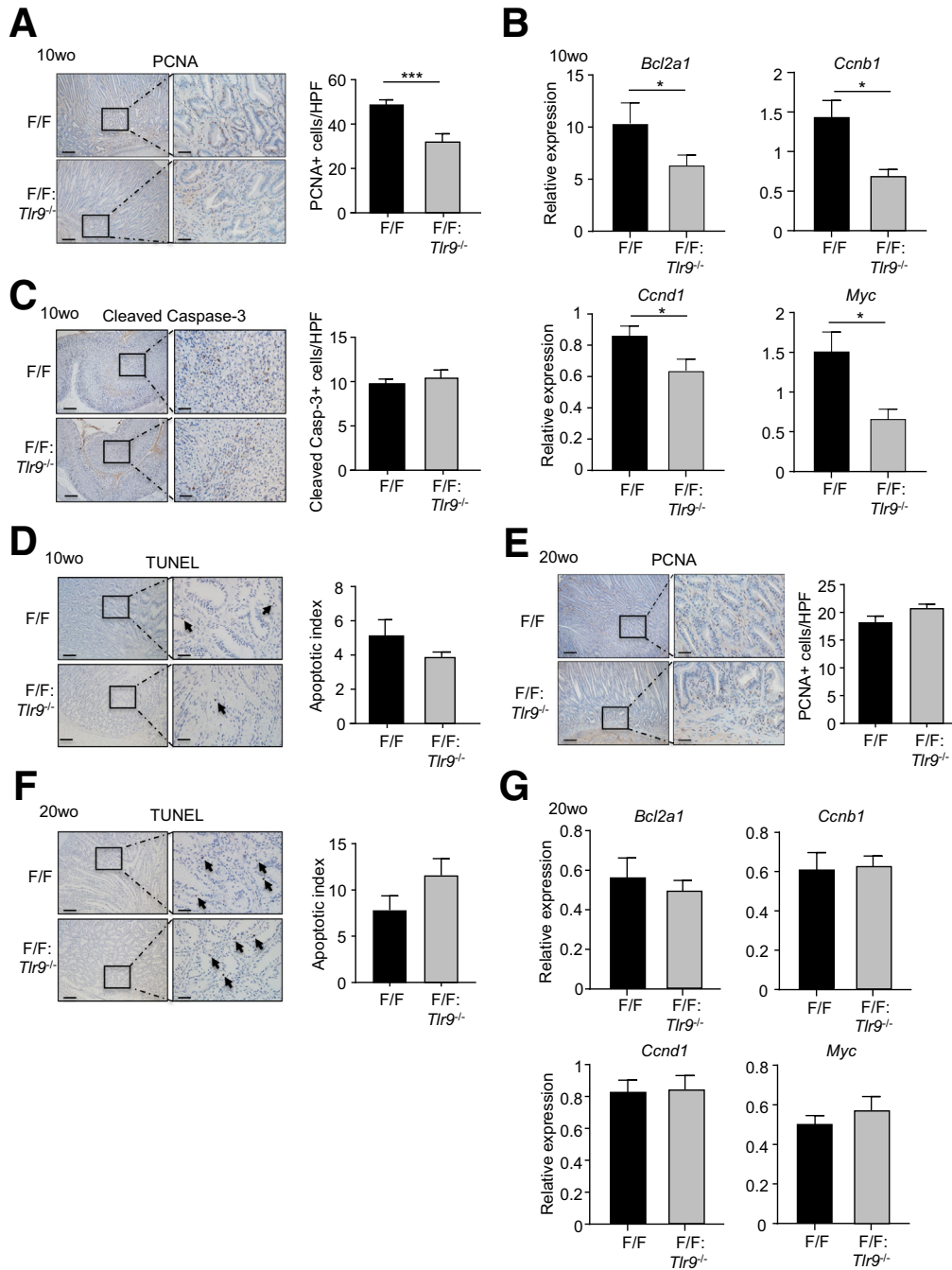


**Figure 4. TLR9 promotes cellular proliferation, but not survival, in tumors of 10-week-old *gp130*<sup>F/F</sup> mice.** (A, C, and D) Representative photomicrographs showing (A) PCNA-stained, (C) cleaved Caspase-3-stained, and (D) TUNEL-stained cross sections under low power (left images) and high power (right images) magnification in gastric tumors from 10-week-old (wo) *gp130*<sup>F/F</sup> (F/F) and F/F:*Tlr9*<sup>-/-</sup> mice. Scale bars: 100  $\mu$ m (left images), 25  $\mu$ m (right images). In (D), arrows point to representative TUNEL-positive stained cells. Also shown are the corresponding graphs depicting quantification of positive cells/high-power field (HPF). n = 6 mice/genotype. \*\*\**P* < .001; unpaired Student *t* tests. (B) qPCR of the indicated cell proliferation genes (all relative to *18s rRNA*) in gastric tumors from 10wo F/F and F/F:*Tlr9*<sup>-/-</sup> mice. n = 6 mice/genotype. \**P* < .05; unpaired Student *t* tests. (E and F) Representative photomicrographs of (E) PCNA-stained and (F) TUNEL-stained cross sections under low power (left images) and high power (right images) magnification of gastric tumors from 20wo F/F and F/F:*Tlr9*<sup>-/-</sup> mice. Scale bars: 100  $\mu$ m (left images), 25  $\mu$ m (right images). In (F), arrows point to representative TUNEL-positive stained cells. Also shown are corresponding graphs depicting positive cells/HPF. n = 6 mice/genotype. (G) qPCR of the indicated cell proliferation genes (all relative to *18s rRNA*) in gastric tumors from 20wo F/F and F/F:*Tlr9*<sup>-/-</sup> mice. n = 6 mice/genotype.

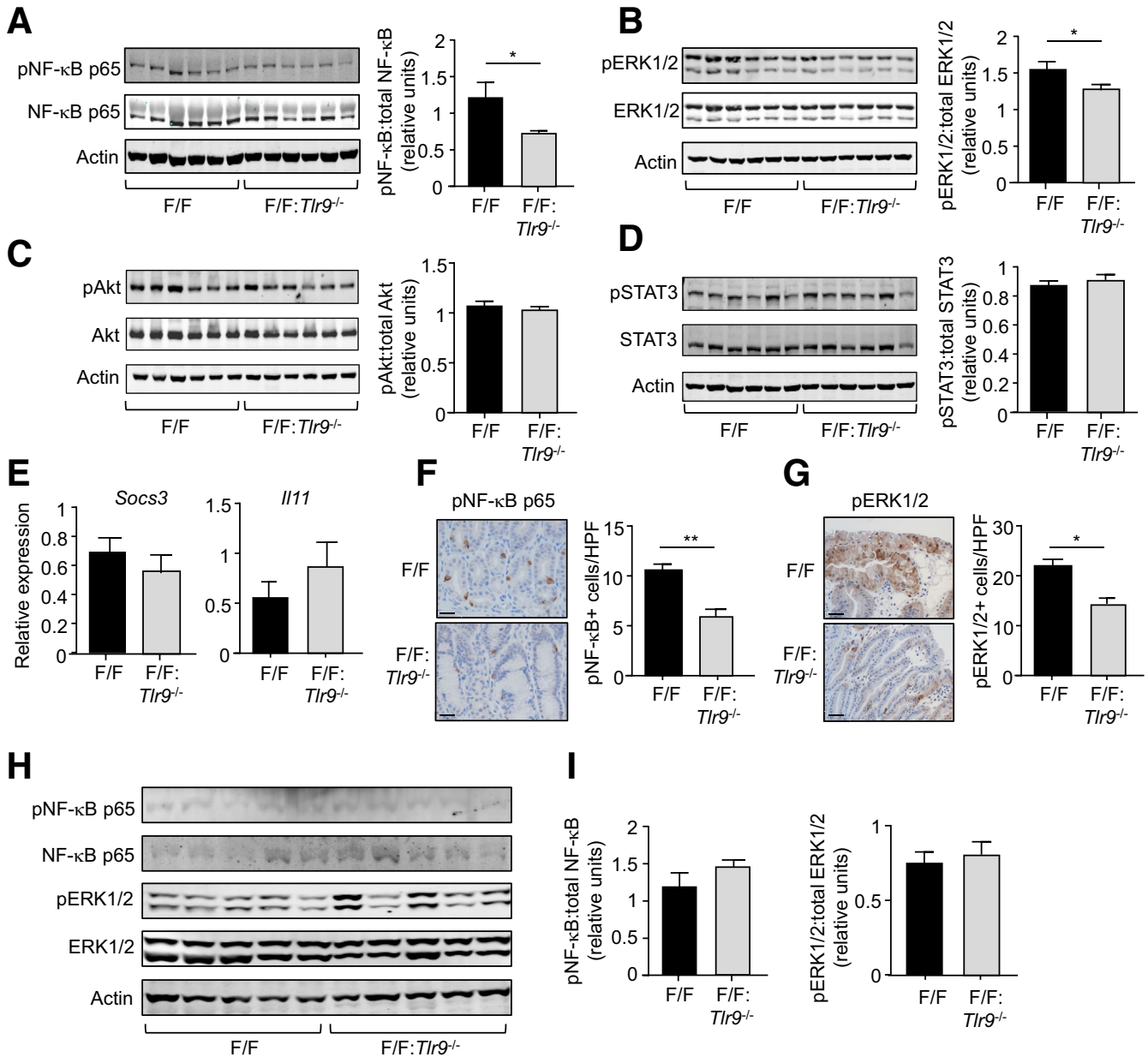


**Figure 5. TLR9 promotes gastric tumorigenesis in 10-week-old *gp130<sup>F/F</sup>* mice through multiple signaling cascades.** (A–D) Western blots of gastric tumor tissue lysates from 10-week-old (wo) *gp130<sup>F/F</sup>* (*F/F*) and *F/F: Tlr9<sup>-/-</sup>* mice with the indicated antibodies. Each lane represents an individual mouse sample. Graphs depict densitometric quantification of relative expression of phosphorylated signaling molecules (ratio of phosphorylated versus total protein) from the corresponding blots on gastric tumor tissue lysates ( $n = 6$  mice/genotype). (E) qPCR of the indicated genes (relative to *18s rRNA*) in gastric tumors from 10wo *F/F* and *F/F: Tlr9<sup>-/-</sup>* mice. (F and G) Representative high power photomicrographs showing immunohistochemical staining of (F) pNF-κB p65 and (G) pERK1/2 in cross sections of gastric tumors from 10wo *F/F* and *F/F: Tlr9<sup>-/-</sup>* mice. Scale bars: 50  $\mu$ m. Graphs depict the corresponding enumeration of positive cells/high power field (HPF).  $n = 6$  mice/genotype. \* $P < .05$ , \*\* $P < .01$ ; unpaired Student *t* test. (H) Western blots of gastric tumor tissue lysates from 20wo *F/F* and *F/F: Tlr9<sup>-/-</sup>* mice with the indicated antibodies. Each lane represents an individual mouse sample. (I) Graphs depict densitometric quantification of the relative expression of phosphorylated signaling molecules (ratio of phosphorylated versus total protein) from the corresponding blots on gastric tumor tissue lysates ( $n = 5$  mice/genotype).

and broth gavaged WT and *Tlr9<sup>-/-</sup>* mice showed that protein levels of pNF-κB p65 and pERK1/2 MAPK were significantly higher in the gastric mucosa of *H felis*-infected WT mice than *H felis*-infected *Tlr9<sup>-/-</sup>* mice, the latter of which were similar

to WT and *Tlr9<sup>-/-</sup>* broth control animals (Figure 7H). Therefore, these data suggest that TLR9-dependent NF-κB and ERK1/2 MAPK signaling pathways contribute to *H felis*-induced gastric pathogenesis in vivo.

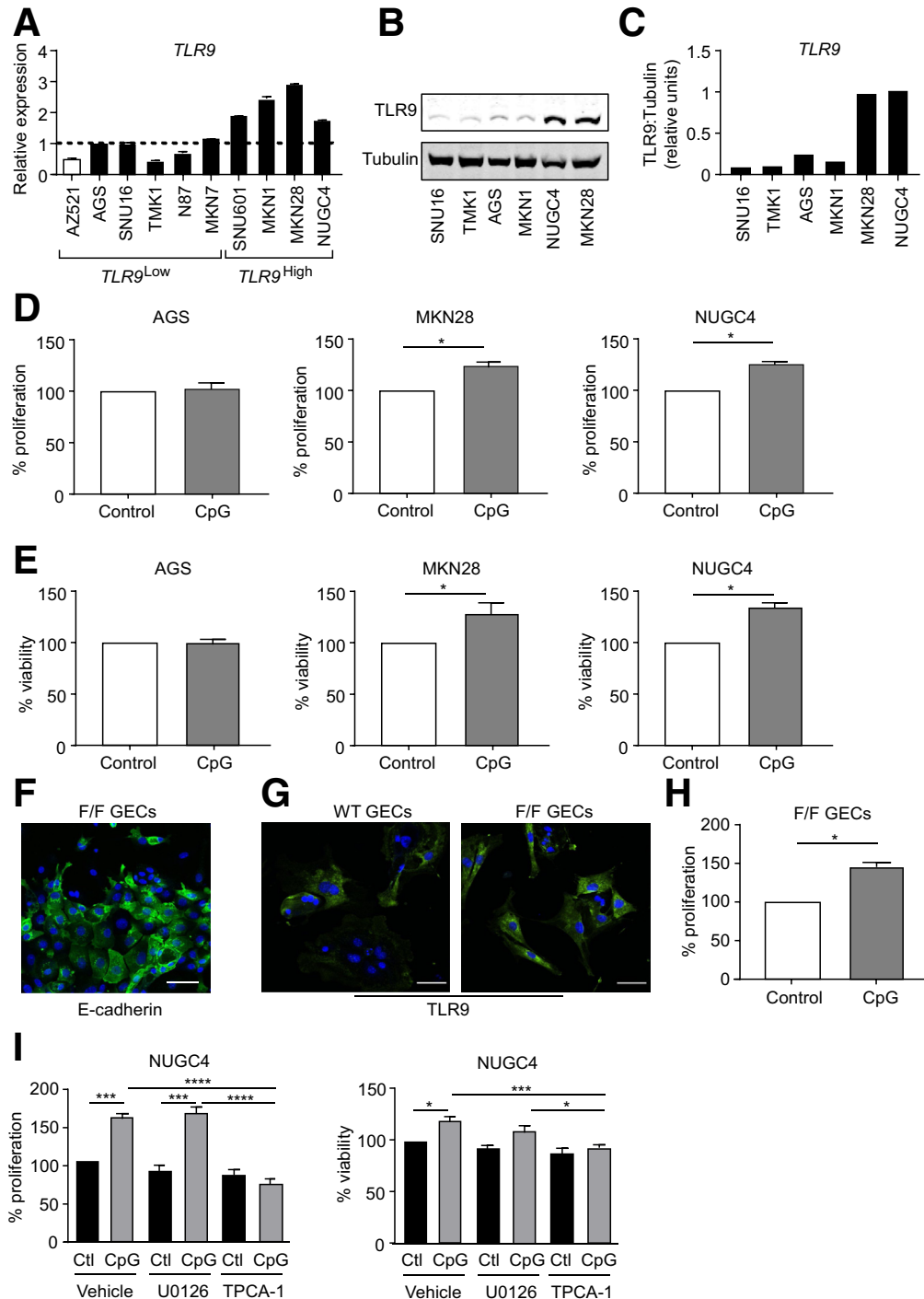


**Figure 6. TLR9 promotes human GC and mouse *gp130*<sup>F/F</sup> primary gastric epithelial cell growth in vitro.** (A) qPCR expression analyses of *TLR9* (normalized to the housekeeping gene *ACTB*) in human GC cell lines (black bars) and a control duodenal cancer cell line (white bar). Expression values were relative to AGS (assigned a value of “1”, and cell lines with a relative expression value above 1 were defined as high expressing for *TLR9*, as depicted by the dotted line). (B) Western blots of lysates from human GC cell lines with the indicated antibodies. (C) Densitometry quantification of *TLR9* protein expression from (B) relative to tubulin. (D and E) Cell proliferation (D) and viability (E) assays of AGS (*TLR9*<sup>Low</sup>), NUGC4 (*TLR9*<sup>High</sup>), and MKN28 (*TLR9*<sup>High</sup>) cells treated with either *TLR9* ligand CpG-DNA (ODN-2006) (2  $\mu$ mol/L) or control oligonucleotide for 24 and 48 hours, respectively. Data are presented from 3 independent experiments. \**P* < .05; paired Student *t* test. (F and G) Representative immunofluorescence images of (F) *gp130*<sup>F/F</sup> (F/F) primary gastric epithelial cells (GECs) stained for E-cadherin and (G) WT and F/F primary GECs stained for *TLR9*. DAPI nuclear staining is blue. Scale bars: 50  $\mu$ m. (H) Proliferation assays of F/F primary GECs treated with either *TLR9* ligand CpG-DNA (ODN-2006) (2  $\mu$ mol/L) or control oligonucleotide for 24 hours. Data are presented from 3 independent experiments. \**P* < .05; paired Student *t* test. (I) Cell proliferation and viability assays of NUGC4 cells pretreated with inhibitors of the NF- $\kappa$ B (TPCA-1) and ERK1/2 MAPK (U0126) pathways before stimulation with CpG DNA (2  $\mu$ mol/L) or control oligonucleotide for 24 and 48 hours, respectively. Data are presented from 3 independent experiments. \**P* < .05, \*\*\**P* < .001, \*\*\*\**P* < .0001; one-way ANOVA.

**Table 2.** Significance Values Were Calculated for *TLR9* Gene Expression (by qPCR) Among *TLR9*<sup>HIGH</sup> (SNU601, MKN1, MKN28, NUGC4) and *TLR9*<sup>LOW</sup> (N87, SNU16, TMK1, AGS, MKN7) Human Gastric Cancer and Duodenal (AZ521; *TLR9*<sup>LOW</sup>) Cell Lines

Cell line comparison <sup>a</sup>	P value <sup>b</sup>
AZ521 vs SNU16	****
AZ521 vs AGS	****
AZ521 vs MKN7	****
AZ521 vs SNU601	****
AZ521 vs MKN1	****
AZ521 vs MKN28	****
AZ521 vs NUGC4	****
N87 vs SNU16	***
N87 vs TMK1	*
N87 vs AGS	***
N87 vs MKN7	****
N87 vs SNU601	****
N87 vs MKN1	****
N87 vs MKN28	****
N87 vs NUGC4	****
SNU16 vs TMK1	****
SNU16 vs SNU601	****
SNU16 vs MKN1	****
SNU16 vs MKN28	****
SNU16 vs NUGC4	****
TMK1 vs AGS	****
TMK1 vs MKN7	****
TMK1 vs SNU601	****
TMK1 vs MKN1	****
TMK1 vs MKN28	****
TMK1 vs NUGC4	****
AGS vs SNU601	****
AGS vs MKN1	****
AGS vs MKN28	****
AGS vs NUGC4	****
MKN7 vs SNU601	****
MKN7 vs MKN1	****
MKN7 vs MKN28	****
MKN7 vs NUGC4	****
SNU601 vs MKN1	****
SNU601 vs MKN28	****
MKN1 vs MKN28	****
MKN1 vs NUGC4	****

<sup>a</sup>Analyses were performed using one-way ANOVA with Tukey multiple comparison test.

<sup>b</sup>\**P* < .05, \*\*\**P* < .001, \*\*\*\**P* < .0001.

Assessment of gastric (antrum and corpus) mucosal cellular proliferation by PCNA and Ki67 immunohistochemical staining confirmed that the hyperproliferative gastric phenotype of WT mice on chronic *H felis* infection was significantly attenuated by TLR9 deficiency (Figure 8A and B). These gastric parameters in *H felis*-infected *Tlr9*<sup>-/-</sup>

mice remained slightly higher than those in *Tlr9*<sup>-/-</sup> control animals, suggesting that TLR9 deficiency led to a partial (albeit significant) reduction in *H felis*-induced gastric hyperplasia. These observations were also confirmed at the molecular level on qPCR gene expression analysis of markers for proliferative stem cells (*Lgr5*),<sup>29</sup> chief cells (*Mist1/Bhlha15*),<sup>30</sup> parietal cells (*Atp4a*),<sup>31</sup> and metaplasia (*Cd44v9*).<sup>32</sup> Specifically, consistent with the suppressed gastric proliferative phenotype of *Helicobacter*-infected *Tlr9*<sup>-/-</sup> mice (versus WT mice), expression of *Lgr5* (increased during *Helicobacter* infection<sup>29</sup>) was significantly down-regulated (~4.5-fold) in infected *Tlr9*<sup>-/-</sup> mice compared with WT mice (Figure 8C). With respect to metaplasia (which usually occurs subsequent to gastritis and associated hyperplasia) of chronic *Helicobacter* infection, gastric *Mist1* expression in chief cells, which is suppressed during metaplasia and dysplasia,<sup>30</sup> was similarly down-regulated (5- to 6-fold) in both WT and *Tlr9*<sup>-/-</sup> mice infected with *Helicobacter* compared with their broth controls (Figure 8D). Also, *Cd44v9* mRNA levels (up-regulated on chronic *Helicobacter* infection and metaplasia<sup>32,33</sup>) were similarly elevated (2- to 3-fold) in both WT and *Tlr9*<sup>-/-</sup> mice infected with *Helicobacter* compared with their broth controls (Figure 8E). Furthermore, consistent with the loss of parietal cells during *Helicobacter* infection and upon metaplasia,<sup>31</sup> mRNA levels of *Atp4a* were similarly down-regulated (~4-fold) in WT and *Tlr9*<sup>-/-</sup> mice infected with *Helicobacter* compared with their broth controls (Figure 8F). Taken together, these molecular changes further support the notion that TLR9 contributes to early proliferative changes in the gastric mucosa, without impacting on lineage differentiation of gastric epithelial progenitors, during *Helicobacter* infection.

The reduced gastric hyperplasia in *H felis*-infected *Tlr9*<sup>-/-</sup> mice was associated with lower gastric inflammation, as evidenced by significantly lower inflammation scores and reduced numbers of infiltrating CD45<sup>+</sup>, B220<sup>+</sup>, and CD3<sup>+</sup> immune cell subsets in the stomachs of *H felis*-infected *Tlr9*<sup>-/-</sup> mice compared with their infected WT counterparts (Figure 9A–D). Similarly, at the molecular level, elevated mRNA levels of inflammatory mediators (ie, *Cxcl1*, *Cxcl2*, *Tnfa*) in *H felis*-infected WT mouse stomachs (compared with broth control WT) were also significantly lower in infected *Tlr9*<sup>-/-</sup> mouse stomachs (Figure 9E). Interestingly, the suppressed gastric inflammation (Figure 9A–D) and hyperplasia (Figure 8A and B) in infected *Tlr9*<sup>-/-</sup> mice occurred despite enhanced *H felis* colonization (Figure 9F and G), which is consistent with the inverse relationship between *H pylori* colonization and gastritis severity observed in the mouse stomach.<sup>34</sup>

## Discussion

In this study, we reveal that the TLR9 endosomal DNA sensor promotes early-stage gastric inflammation-associated carcinogenesis. In this respect, our findings are consistent with accumulating evidence for the contribution of TLR9 to the pathogenesis of various cancers (eg, pancreatic cancer, esophageal cancer).<sup>13–17</sup> For example, in

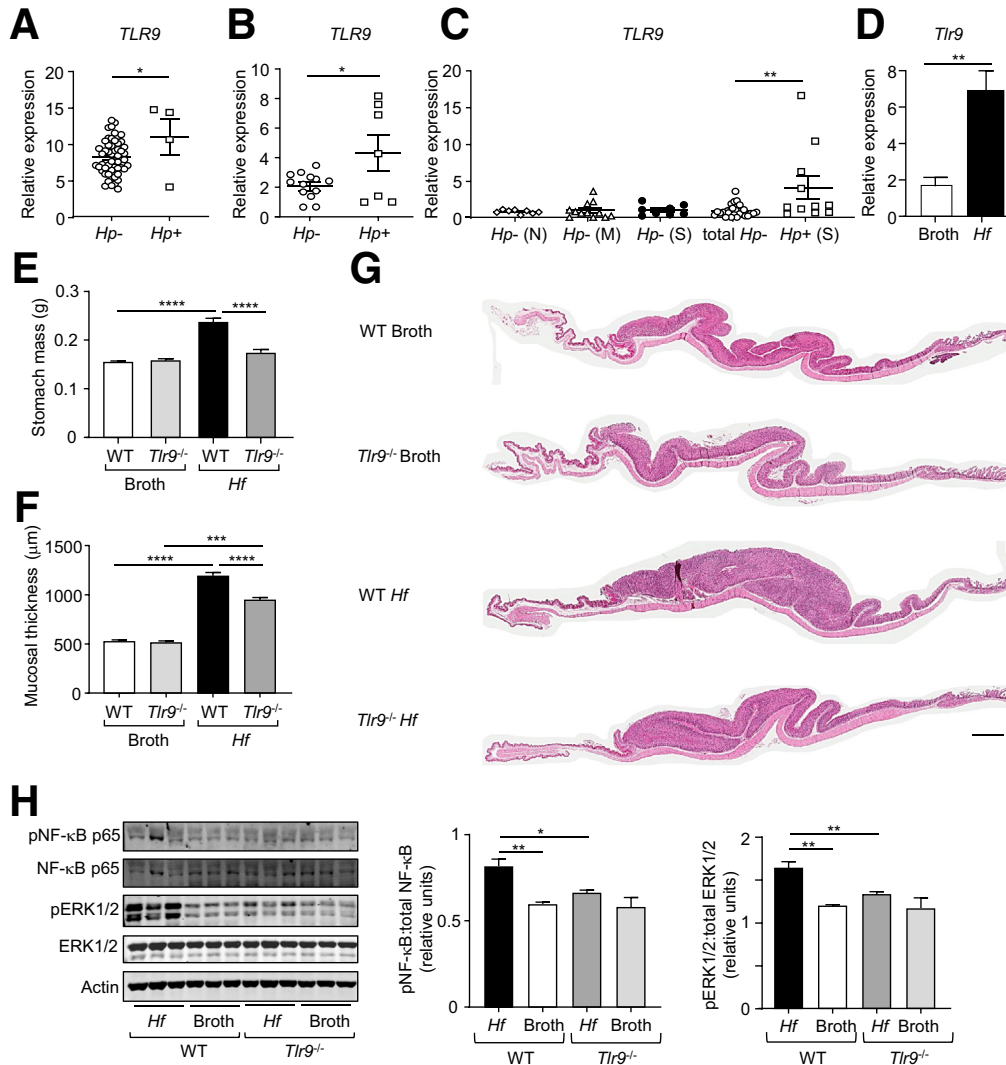


**Figure 7. TLR9 is up-regulated in human *H pylori*-infected and mouse *H felis*-infected gastric tissues, and *H felis*-induced gastric hyperplasia is suppressed in TLR9-deficient mice.** (A and B) Gene expression of *TLR9* in gastric tumors from (A) TCGA intestinal-type GC patients (*Hp*<sup>-</sup>, *n* = 53; *Hp*<sup>+</sup>, *n* = 4), and (B) Australian/Chinese GC patients (*Hp*<sup>-</sup>, *n* = 13; *Hp*<sup>+</sup>, *n* = 7), based on their *H pylori* (*Hp*) status. \**P* < .05; unpaired Student *t* test. (C) qPCR expression of *TLR9* (relative to *18S rRNA*) in gastric tissues from GC-free individuals, based on the *H pylori* status (*Hp*<sup>-</sup> normal (N), *n* = 8; *Hp*<sup>-</sup> mild gastritis (M), *n* = 12; *Hp*<sup>-</sup> severe gastritis (S), *n* = 8; total *Hp*<sup>-</sup>, *n* = 28; *Hp*<sup>+</sup> severe gastritis (S), *n* = 11). \*\**P* < .01; one-way ANOVA. (D) qPCR expression of *Tlr9* (relative to *18s rRNA*) in gastric body tissues from WT mice at 4 months after oral gavage with either broth or *H felis* (*Hf*). *n* = 6 mice/group. \*\**P* < .01; unpaired Student *t* test. (E and F) Shown are (E) stomach weights and (F) mucosal thicknesses of WT and *Tlr9*<sup>-/-</sup> mice at 4 months after oral gavage with either broth or *H felis* (*n* = 12 mice/group). (G) Representative photomicrographs showing H&E-stained whole slide scans of stomachs. Scale bars: 1 mm. (H) Western blots of gastric body tissue lysates from *Tlr9*<sup>-/-</sup> and WT mice at 4 months after oral gavage with either broth or *H felis* with the indicated antibodies. Graphs depict densitometry quantification of the indicated phosphorylated signaling molecules shown in the Western blots (*n* = 3 lysates/group), and relative expression was determined against the corresponding amount of total protein. \**P* < .05, \*\**P* < .01; one-way ANOVA.

pancreatic cancer, TLR9 has distinct pro-tumorigenic effects on epithelial, immune/inflammatory, and fibroblastic cells, which collectively fuel an inflamed tumor microenvironment (TME) during early disease onset that supports the neoplastic outgrowth of the transformed epithelium.<sup>13</sup> Regarding the former, our findings here demonstrate that TLR9 elicits proliferative responses on the gastric epithelium during early-stage tumorigenesis, which is coincident with its transcriptional up-regulation in the gastric (tumor)

epithelium, but not immune cell-containing stroma, of 12-week-old (early onset of tumorigenesis) versus 24-week-old (late established tumorigenesis) *gp130*<sup>F/F</sup> mice. These observations support the notion that in cancers (eg, pancreatic, gastric) whose initiation is reliant on tumor-promoting pro-inflammatory signals, TLR9-driven epithelial (tumor) cell growth, either directly or indirectly via activation of immune cells within the TME, outweighs TLR9-mediated adaptive immune-based anti-tumor immunity that

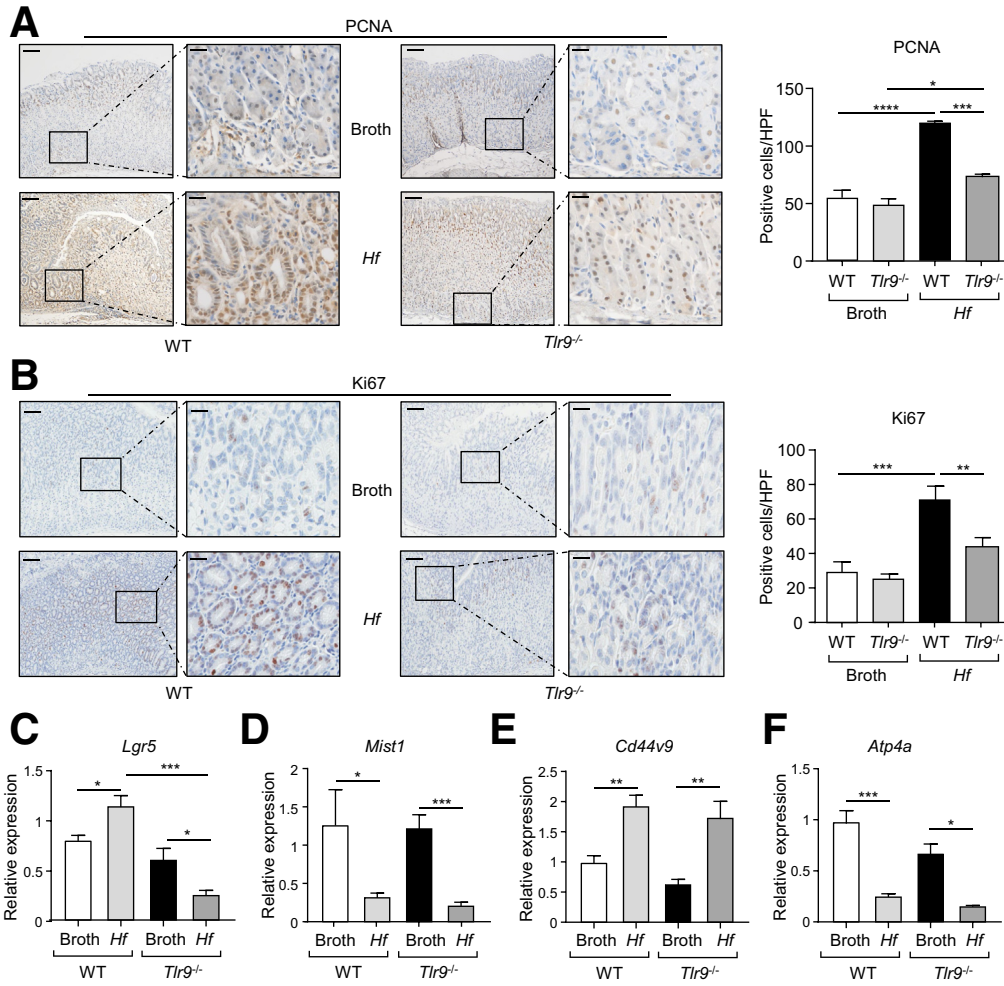


**Figure 8. Reduced expression levels of cellular and molecular markers of proliferation in *H felis*-infected TLR9-deficient mice.** (A and B) Shown are (A) PCNA-stained and (B) Ki67-stained cross sections under low power (left images) and high power (right images) magnification of the corpus (body) region of stomachs from WT and *Tlr9*<sup>-/-</sup> mice challenged with either broth or *H felis*. Graphs depict enumeration of positive cells/high power field (HPF). Scale bars: 100 μm (left images) and 25 μm (right images). \**P* < .05, \*\**P* < .01, \*\*\**P* < .001, \*\*\*\**P* < .0001; one-way ANOVA. (C–F) qPCR expression analyses of the indicated genes (after normalization for 18S rRNA) in gastric body tissues from WT and *Tlr9*<sup>-/-</sup> mice at 4 months after oral gavage with either broth or *H felis* (*Hf*) (n = 5 mice/group). \**P* < .05, \*\**P* < .01, \*\*\**P* < .001; one-way ANOVA.

has been described in certain cancer types (eg, brain, colon).<sup>19,35–37</sup> The complex role of TLR9 in cancer is also evidenced by observations that TLR9 exhibits both tumor-promoting and tumor suppressive activities within a specific cancer type such as glioma.<sup>37,38</sup> The mechanistic basis for these contrasting pro- and anti-tumorigenic effects of TLR9 remains unclear. However, it is likely to involve differences in the temporal (ie, early versus late stage) expression pattern of TLR9, as well as the cell types (eg, epithelial, immune) in which TLR9 is predominantly expressed, the latter of which is influenced by the highly heterogeneous TME among cancers.

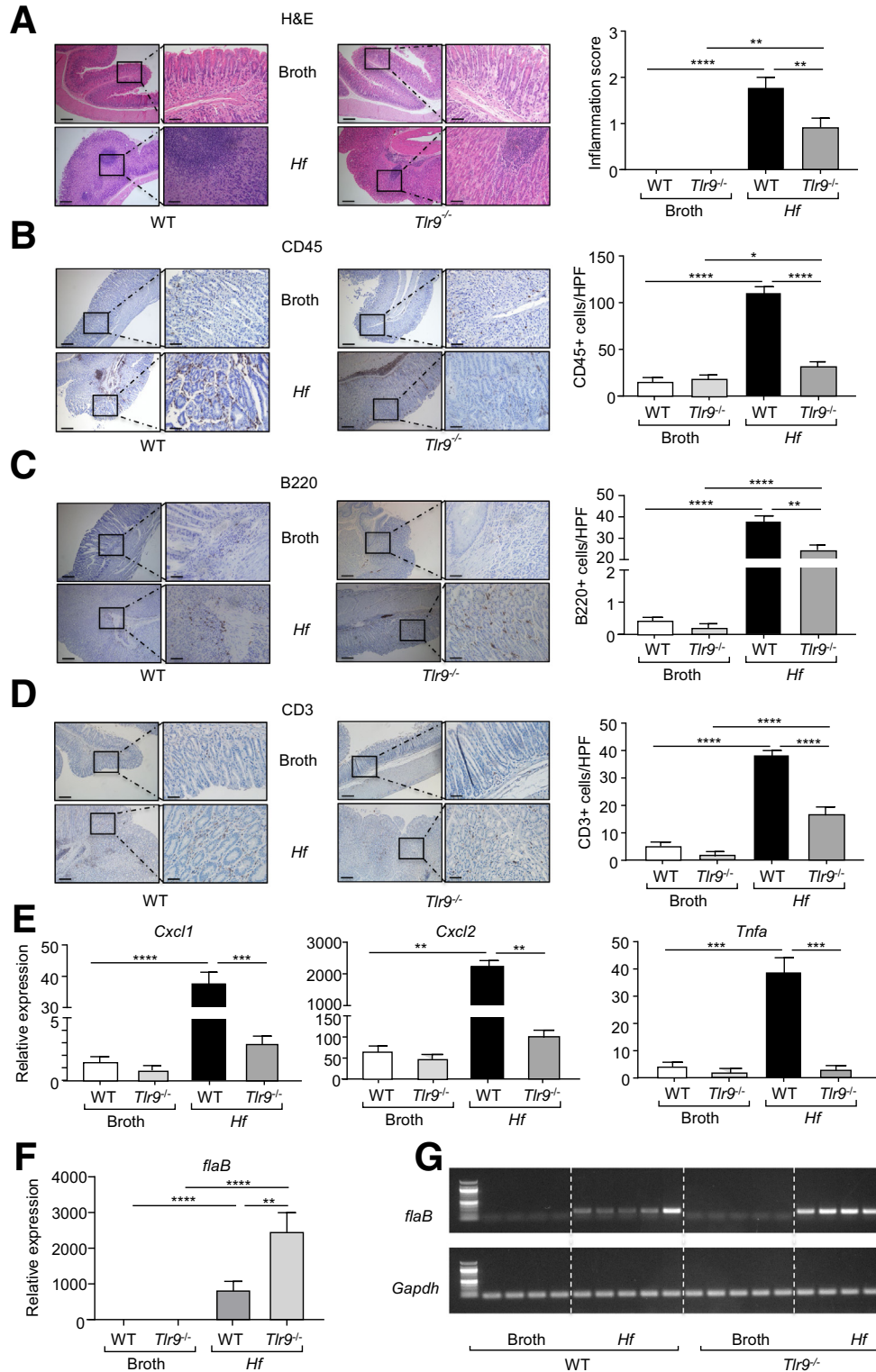
The opposing roles of TLR9 in cancer also extend to contrasting observations on its pro- or anti-inflammatory activities in the pathogenesis of *Helicobacter*-induced gastritis. For instance, in a 3-week *H felis* infection mouse model, TLR9 elicited a pro-inflammatory response as evidenced by reduced numbers of infiltrating neutrophils in the gastric mucosa of infected *Tlr9*<sup>-/-</sup> mice.<sup>23</sup> Importantly, our current study builds on this observation by demonstrating a causal role for TLR9 in promoting chronic *H felis*-induced gastric pathology, incorporating gastritis and gastric epithelial hyperplasia that are aligned with the

initiating stages of *H pylori*-induced human GC.<sup>2,3</sup> However, conversely, an anti-inflammatory role for TLR9 has been assigned during early phases of *H pylori* infection, whereby *Tlr9*<sup>-/-</sup> mice displayed elevated gastric neutrophil infiltration within 6–8 weeks after *H pylori* (SS1 and PMSS1 strains) infection.<sup>21,22</sup> Although TLR9-mediated recognition of *H pylori* DNA is likely to be one mechanism by which *Helicobacter* species can hijack TLR9-dependent cellular responses in the host,<sup>39,40</sup> the reason for the contrasting roles reported for TLR9 in *Helicobacter*-induced inflammatory responses is less clear but may involve differences in study design relating to the genetic backgrounds of mouse strains, variations within the gut microbiota observed among animal facilities, and/or strains of *Helicobacter* used (eg, *H pylori* SS1, *H pylori* PMSS1, *H felis*).<sup>21–23</sup>

It is also noteworthy to compare our findings on the role of TLR9 in promoting the early initiating stages of GC with those of other TLR family members, among which TLR2 is best characterized for its prominent role in driving the growth of established tumors in later stages of GC.<sup>7,8,11</sup> A likely explanation for the differential roles of TLR2 and TLR9 in GC is that TLR2 drives tumorigenesis by directly augmenting proliferation and suppressing apoptosis of the

**Figure 9. Genetic ablation of *Tlr9* reduces *H felis*-induced gastric inflammation.**

(A–D) Representative photomicrographs showing (A) H&E-stained, (B) CD45-stained, (C) B220-stained, and (D) CD3-stained cross sections under low power (left images) and high power (right images) magnification through the body of stomachs from *Tlr9*<sup>-/-</sup> and WT mice at 4 months after oral gavage with either broth or *H felis*. Also shown are the corresponding graphs depicting (A) the inflammation scores or (B–D) positive cells/high power field (HPF). Scale bars: 200 μm (left images) and 50 μm (right images). n = 6 mice/group. \**P* < .05, \*\**P* < .01, \*\*\*\**P* < .0001; one-way ANOVA. (E) qPCR expression of representative inflammatory genes (relative to *18s rRNA*) in gastric corpus (body) tissues from the stomachs of WT and *Tlr9*<sup>-/-</sup> mice at 4 months after oral gavage with either broth or *H felis*. n = 6 mice/group. \*\**P* < .01, \*\*\**P* < .001, \*\*\*\**P* < .0001; one-way ANOVA. (F and G) In (F), qPCR expression of *H felis flaB* (relative to *Gapdh*), and (G) representative agarose gel of reverse transcription PCR of *H felis flaB* along with *Gapdh*, in stomachs from WT and *Tlr9*<sup>-/-</sup> mice at 4 months after oral gavage with either broth or *H felis*. n = 6 mice/group. \*\**P* < .01, \*\*\*\**P* < .0001; one-way ANOVA.



transformed gastric epithelium, independent of its expression in immune cells (eg, bone marrow-derived myeloid lineage) and intratumoral inflammation.<sup>8,11</sup> Furthermore, TLR2, unlike TLR9 (K.T. and B.J.J., unpublished data), is transcriptionally up-regulated in the transformed gastric

epithelium by the latent oncogenic transcription factor STAT3, whose hyperactivation is a feature of >50% of human GC cases and drives tumorigenesis in the *gp130*<sup>F/F</sup> model, the latter of which mimics many of the molecular and cellular features of human GC, including that associated

with *Helicobacter* infection.<sup>8,25,41</sup> Although the mechanism by which TLR9 is transcriptionally up-regulated in gastric inflammation-associated tumorigenesis is currently unknown, it is likely to involve NF- $\kappa$ B, whose dysregulated activation is a common feature of gastric tumorigenesis and *Helicobacter* infection.<sup>42,43</sup> In addition, a single nucleotide polymorphism within the TLR9 promoter (TLR9-1237T/C), which increases *TLR9* transcriptional activity in response to NF- $\kappa$ B, is associated with increased risk of *H pylori*-mediated premalignant changes in the gastric epithelium.<sup>44</sup> These findings are in concordance with our current study, in which we observed elevated *Tlr9* mRNA levels in early, but not late, stage *gp130<sup>F/F</sup>* gastric tumors, which aligned with the high and very low levels of NF- $\kappa$ B activity in early and late stage gastric tumors, respectively.

In conclusion, our study defines a key role for TLR9 in the initiating stage of gastric inflammation-associated tumorigenesis (including that caused by *Helicobacter* infection), whereby up-regulation of TLR9 promotes the proliferative outgrowth of gastric epithelial cells. In the *gp130<sup>F/F</sup>* GC model, TLR9 deficiency led to the selective suppression of early initiation (10-week-old mice), but not later establishment and progression (20-week-old mice), stage of gastric tumorigenesis by transiently impairing the proliferative potential of the gastric epithelium, as well as immune cell infiltration in the TME. These observations aligned with reduced NF- $\kappa$ B (and to a lesser extent, ERK MAPK) activity on TLR9 deficiency in early (but not late) stage *gp130<sup>F/F</sup>* tumors, when TLR9 is also significantly up-regulated. Because activation of NF- $\kappa$ B (but not ERK MAPK) also associated with the TLR9-driven proliferative responsiveness of human GC cells, we propose that up-regulation of TLR9 in the gastric epithelium and concomitant preferential activation of NF- $\kappa$ B is an important step in the early stages of gastric tumorigenesis. Interestingly, because NF- $\kappa$ B is also a potent inducer of inflammatory responses, it is possible that TLR9 engages with NF- $\kappa$ B (and potentially other pathways) to also induce early inflammatory responses in the gastric compartment. We also note that in the later establishment and progression stages of gastric tumorigenesis, the chronic inflamed TME overrides the initial TLR9-driven activities on gastric epithelial and immune cells, thus promoting tumor progression independent of TLR9. In this regard, elevated *Tlr9* mRNA levels in the stroma-enriched non-tumor versus tumor tissues of 24-week-old *gp130<sup>F/F</sup>* mice are likely a consequence of the sustained presence of TLR9-expressing immune cell infiltrates in the highly inflamed gastric TME of 24-week-old *gp130<sup>F/F</sup>* mice. Moreover, our study raises the intriguing question of the relative contribution of TLR9 expression and activation in gastric epithelial versus immune cells to the pathogenesis of gastric inflammation and carcinogenesis. Although the host gastric epithelium is the first line of defense against *H pylori*, macrophages are critical facilitators of the early gastric inflammatory response to *H pylori*, whereby upon their recruitment to the infected gastric mucosa, they are subsequently infected by *H pylori*, leading to their activation, which facilitates the recruitment and activation of additional inflammatory cells (eg, macrophages themselves,

neutrophils, dendritic cells).<sup>45–48</sup> Indeed, our observation that TLR9 is expressed in both gastric epithelial and immune cell-enriched stroma compartments, albeit at markedly reduced levels in the latter, supports the notion that although the tumor-promoting mechanisms of TLR9 are primarily mediated by its direct epithelial cell regulation, other mechanisms, for instance those impacting immune cell function, might also operate. Therefore, future reciprocal bone marrow chimera studies in both *gp130<sup>F/F</sup>* and *H felis* infection models will play a pivotal role in elucidating the relative contribution of TLR9-expressing bone marrow-derived hematopoietic (ie, immune) cells to gastric disease pathogenesis. We also note that our findings pave the way for future studies to investigate the role of the microbiome in triggering TLR9-induced gastric inflammation-associated tumorigenesis, for instance by comparing the extent of gastric tumorigenesis in germ-free *gp130<sup>F/F</sup>* versus *gp130<sup>F/F</sup>:Tlr9<sup>-/-</sup>* mice, and/or specific pathogen-free *gp130<sup>F/F</sup>* versus *gp130<sup>F/F</sup>:Tlr9<sup>-/-</sup>* mice treated with broad-spectrum antibiotics to eliminate gastric microbes.

## Methods

### Human Biopsies

Snap-frozen and formalin-fixed gastric tissue biopsies were collected from GC or GC-free patients enrolled at Monash Medical Centre (Melbourne, Australia) and Xin Hua Hospital (Shanghai, China) undergoing surgical resection or upper gastrointestinal endoscopy (Table 1). Patients with a history of taking nonsteroidal anti-inflammatory drugs, proton pump inhibitors, or antibiotics were excluded. Histopathologic assessment and *H pylori* status were determined as before.<sup>49</sup> Full and informed patient consent was obtained, and biopsy collections were approved by the Monash Health Human Research Ethics Committee and Xin Hua Hospital Ethics Committee.

### Mouse Strains

The *gp130<sup>F/F</sup>* and *Tlr9<sup>-/-</sup>* mice (the latter donated by S. Summers, Monash University, Australia) have been described previously and were used to generate *gp130<sup>F/F</sup>:Tlr9<sup>-/-</sup>* mice.<sup>50,51</sup> All mice were on a mixed 129Sv $\times$ C57BL/6 background, and where possible equal numbers of male and female mice were used. Genetically matched and age-matched littermates, including WT controls, were included in all experiments. Mice were housed under specific pathogen-free conditions on a 12-hour light/dark cycle. All animal experiments were approved by the Monash University Monash Medical Centre “B” Animal Ethics Committee.

### *H felis* Infection Model

*H felis* (strain CS1) was cultured on horse blood agar (Oxoid, Nepean, Canada) and then harvested and cultured in brain heart infusion broth (Oxoid) to yield *H felis* suspensions for mouse inoculation.<sup>52,53</sup> WT and *Tlr9<sup>-/-</sup>* male and female mice aged 4–6 weeks were randomly administered with a single 100  $\mu$ L aliquot of either control brain heart infusion broth or  $2 \times 10^7$  *H felis* bacteria by oral gavage and then culled after 4 months.<sup>53,54</sup> Gastric colonization of

*H. felis* was confirmed by qPCR amplification of the *H. felis* flagellar filament B (*flaB*) gene using the following primer sequences<sup>55</sup>: *FlaB* Forward 5'-TCGATTGGTCCTA-CAGGCTCAGA-3', *FlaB* Reverse 5'-TTCTTGTGATGACATTGACCAACGCA-3'.

### Histology, Immunohistochemistry, and Immunofluorescence

Formalin-fixed and paraffin-embedded mouse gastric tissue sections were stained with hematoxylin-eosin for histologic assessment. The extent of inflammation was blindly scored 0 (none), 1 (mild), 2 (moderate), and 3 (severe) independently by 2 authors, and the average was determined. Apoptosis was assessed by the terminal deoxynucleotidyl transferase (tdT)-mediated dUDP nick-end labeling (TUNEL) assay (Millipore, Burlington, MA), as well as immunohistochemistry with an anti-cleaved Caspase-3 antibody (1:100 dilution) (Cell Signaling Technology, Danvers, MA). Immunohistochemistry was also performed to evaluate cell proliferation with an antibody against PCNA (1:5000 dilution) (Cell Signaling Technology), inflammatory cell infiltrates with antibodies against CD45, B220, and CD3 (each at 1:100 dilution) (BD Biosciences, Franklin Lakes, NJ), and activation of signaling pathways with antibodies against phosphorylated (p)Ser<sup>536</sup>-p65 NF- $\kappa$ B and pThr<sup>202</sup>/pTyr<sup>204</sup>-ERK1/2 (each at 1:100 dilution) (Cell Signaling Technology). To quantify staining, digital images of photomicrographs (40 $\times$  magnification) were viewed using ImageJ software (National Institutes of Health, Bethesda, MD),<sup>56</sup> and positive-staining cells were counted manually (n = 20 fields/section) and in a blinded manner. Immunofluorescence was performed with antibodies against TLR9 (AbCam, Cambridge, UK) at 1:50 dilution followed by Alexa Fluor 488 anti-rabbit secondary (Invitrogen, Waltham, MA) at 1:1000 dilution and conjugated E-cadherin Alexa Fluor 488 (Cell Signaling Technology) at 1:100 dilution. Nuclear staining was achieved using 4',6-diamidino-2-phenylindole (DAPI). Sections that underwent the above staining protocol without primary antibodies acted as negative controls. Images were acquired using a Nikon C1 confocal microscope.

### Cell Culture

Human GC cell lines AGS (American Type Culture Collection), MKN28 and NUGC4 (Japanese Collection of Research Bioresources Cell Bank) were grown in Gibco RPMI medium containing 10% fetal calf serum, 1% penicillin-streptomycin, and 1% L-glutamine (Thermo Fisher Scientific, Waltham, MA). Cell lines were characterized and authenticated via short tandem repeat profiling (PowerPlex HS16 System kit; Promega, Madison, WI) and were passaged for under 6 months after receipt in 2013. Cell lines were routinely tested for mycoplasma contamination using the MycoAlert PLUS Mycoplasma Detection Kit (Lonza, Basel, Switzerland). Primary gastric epithelial cells from *gp130*<sup>F/F</sup> mice were generated and cultured using established protocols.<sup>57</sup>

### RNA Isolation and Gene Expression Analyses

Total RNA was isolated from snap-frozen human and mouse gastric tissues and cultured human GC cell lines using TRI Reagent Solution (Sigma-Aldrich, St Louis, MO), followed by on-column rNeasy Mini Kit RNA clean-up and dNase treatment (Qiagen, Hilden, Germany). RNA was transcribed using the Transcriptor High Fidelity cDNA Synthesis Kit (Roche, Basel, Switzerland). qPCR was performed using the 7900HT Fast RT-PCR System (Applied Biosystems, Waltham, MA), and data were acquired and analyzed as before.<sup>8,11</sup> Total RNA and qPCR analyses were performed on laser microdissected mouse gastric tissues as described before.<sup>58</sup> Human (h) *TLR9* and mouse (m) *Tlr9* gene primer sequences are as follows, and for other genes primer sequences are available on request or have been previously published<sup>8,11,31,32,57,58</sup>: h*TLR9* Forward 5'-GTGACAGATCCAAGGTGAAGT-3', h*TLR9* Reverse 5'-CTTCCTCTACAAATGCATCACT-3'; m*TLR9* Forward 5'-ACTGAGCACCCCTGCTTCTA-3', m*TLR9* Reverse 5'-AGATTAGTCAGCGGCAGGAA-3'; m*Gapdh* Forward 5'-CATGGCCTTCCGTGTTCTA-3'.

### Protein Expression Analysis

Immunoblots were performed with antibodies against TLR9 (1:500 dilution) (Abcam), pSer<sup>536</sup>-p65 NF- $\kappa$ B, pThr<sup>202</sup>/pTyr<sup>204</sup>-ERK1/2, pSer<sup>473</sup>-Akt, pTyr<sup>705</sup>-STAT3, total STAT3, total p65 NF- $\kappa$ B, total ERK1/2, total Akt (each at 1:1000 dilution) (Cell Signaling Technology) and Actin (1:1000 dilution) (Sigma-Aldrich). Membranes were analyzed using the Odyssey CLx Imaging System (Li-Cor, Lincoln, NE), and protein expression was quantified as before.<sup>8,11</sup> An ELISA kit to detect tumor necrosis factor  $\alpha$  (BD Biosciences) in gastric tissue lysates was used according to manufacturer's instructions.

### Cell Proliferation and Viability Assays

AGS, NUGC4, MKN28, and *gp130*<sup>F/F</sup> primary gastric epithelial cells (2  $\times$  10<sup>3</sup>) were seeded in triplicate wells in 96-well plates. After 24 hours of serum starvation, cells were treated with either ODN 2006 CpG oligonucleotide (Class B) or ODN 2006 control oligonucleotide (Invivogen, San Diego, CA) for 24 hours (proliferation) or 48 hours (viability). Where indicated, cells were also pretreated for 30 minutes with specific inhibitors against the ERK MAPK (U0126; 0.5  $\mu$ mol/L; Cell Signaling Technology) and NF- $\kappa$ B (TPCA-1; 10  $\mu$ mol/L; Selleck Chemicals, Houston, TX) pathways before stimulation with CpG or control oligonucleotides (both at 2  $\mu$ mol/L). Cell proliferation was assessed with the ClickIT EdU Microplate Assay (Molecular Probes, Eugene, OR) and cell viability by using the MTT assay.<sup>8,11</sup>

### Human Gastric Cancer Patient Datasets

Gene expression data and clinical information from TCGA 18 intestinal-type GC cases with paired tumor and adjacent non-tumor tissue (Table 1), as well as 57 intestinal-type GC cases classified into *H. pylori*-negative or -positive (Table 3), were obtained from TCGA data portal (<https://portal.gdc.cancer.gov/projects/TCGA-STAD>). We used

**Table 3.** Clinicopathologic Features and Demographics of The Cancer Genome Atlas (TCGA) Intestinal-type Gastric Cancer Patient Cohorts Used for TLR9 Expression Profiling Based on *H pylori* Status

	<i>Hp</i> -negative	<i>Hp</i> -positive
Mean age		
Years (range)	66.6 (44–90)	61.3 (45–78)
Sex, n (%)		
Male	35 (66)	3 (75)
Female	18 (34)	1 (25)
Tumor grade, n (%)		
1	10 (18.9)	0
2	18 (34)	3 (75)
3	23 (43.3)	0
4	2 (3.8)	1 (25)

*Hp*, *H pylori*.

reads/kilobase of exon model/million mapped reads to quantify *TLR9* gene expression levels from RNA sequencing data generated from each GC patient.

The Gastric Cancer Project“08-- Singapore Patient Cohort (GSE15459) dataset (Table 1) was sourced for *TLR9* gene expression profiling and overall survival analyses as described previously.<sup>10,23</sup>

### Statistics

All statistical analyses were performed using GraphPad Prism V8.0.2 (San Diego, CA) software. Data normality was assessed using the Agostino and Pearson omnibus K2 normality test, and the appropriate tests to identify statistical significance ( $P < .05$ ) between the means of 2 or multiple groups are presented in the relevant figure legends. All data in figures are expressed as the mean  $\pm$  standard error of the mean from at least 3 technical replicates. The log-rank test was used to calculate the statistical significance of the difference in survival between 2 groups.

### References

- Bray F, Ferlay J, Soerjomataram I, Siegel RL, Torre LA, Jemal A. Global cancer statistics 2018: GLOBOCAN estimates of incidence and mortality worldwide for 36 cancers in 185 countries. *CA Cancer J Clin* 2018; 68:394–424.
- Crew KD, Neugut AI. Epidemiology of gastric cancer. *World J Gastroenterol* 2006;12:354.
- Wroblewski LE, Peek RM Jr, Wilson KT. *Helicobacter pylori* and gastric cancer: factors that modulate disease risk. *Clin Microbiol Rev* 2010;23:713–739.
- Castaño-Rodríguez N, Kaakoush NO, Mitchell HM. Pattern-recognition receptors and gastric cancer. *Front Immunol* 2014;5:336.
- Chmiela M, Karwowska Z, Gonciarz W, Allushi B, Stacek P. Host pathogen interactions in *Helicobacter pylori* related gastric cancer. *World J Gastroenterol* 2017; 23:1521–1540.
- Neill LA, Golenbock D, Bowie AG. The history of toll-like receptors: redefining innate immunity. *Nat Rev Immunol* 2013;13:453–460.
- West AC, Jenkins BJ. Inflammatory and non-inflammatory roles for toll-like receptors in gastrointestinal cancer. *Curr Pharm Des* 2015;21:2968–2977.
- Tye H, Kennedy CL, Najdovska M, Mcleod L, McCormack W, Hughes N, Dev A, Sievert W, Ooi CH, Ishikawa TO, Oshima H, Bhathal PS, Parker AE, Oshima M, Tan P, Jenkins BJ. STAT3-driven upregulation of TLR2 promotes gastric tumorigenesis independent of tumor inflammation. *Cancer Cell* 2012; 22:466–478.
- Man SM, Jenkins BJ. Context-dependent functions of pattern recognition receptors in cancer. *Nat Rev Cancer* 2022. <https://doi.org/10.1038/s41568-022-00462-5>.
- Castaño-Rodríguez N, Kaakoush NO, Pardo AL, Goh KL, Fock KM, Mitchell HM. Genetic polymorphisms in the toll-like receptor signalling pathway in *Helicobacter pylori* infection and related gastric cancer. *Hum Immunol* 2014; 75:808–815.
- West AC, Tang K, Tye H, Yu L, Deng N, Najdovska M, Lin SJ, Balic JJ, Okochi-Takada E, McGuirk P, Keogh B, McCormack W, Bhathal PS, Reilly M, Oshima M, Ushijima T, Tan P, Jenkins BJ. Identification of a TLR2-regulated gene signature associated with tumor cell growth in gastric cancer. *Oncogene* 2017;36: 5134–5144.
- Belmont L, Rabbe N, Antoine M, Cathelin D, Guignabert C, Kurie J, Cadranet J, Wislez M. Expression of TLR9 in tumor-infiltrating mononuclear cells enhances angiogenesis and is associated with a worse survival in lung cancer. *Int J Cancer* 2014;134:765–777.
- Zambirinis CP, Levie E, Nguy S, Avanzi A, Barilla R, Xu Y, Seifert L, Daley D, Greco SH, Deutsch M, Jonnadula S, Torres-Hernandez A, Tippens D, Pushalkar S, Eisenthal A, Saxena D, Ahn J, Hajdu C, Engle DD, Tuveson D, Miller G. TLR9 ligation in pancreatic stellate cells promotes tumorigenesis. *J Exp Med* 2015; 212:2077–2094.
- Ilvesaro JM, Merrell MA, Li L, Wakchoure S, Graves D, Brooks S, Rahko E, Jukkola-Vuorinen A, Vuopala KS, Harris KW, Selander KS. Toll-like receptor 9 mediates CpG oligonucleotide-induced cellular invasion. *Mol Cancer Res* 2008;6:1534–1543.
- Zhang Y, Wang Q, Ma A, Li Y, Li R, Wang Y. Functional expression of TLR9 in esophageal cancer. *Oncol Rep* 2014;31:2298–2304.
- Dai Q, Li XP, Chai L, Long HA, Yang ZH. Polymorphisms of toll-like receptor 9 are associated with nasopharyngeal carcinoma susceptibility. *Tumour Biol* 2014; 35:3247–3253.
- Wang C, Cao S, Yan Y, Ying Q, Jiang T, Xu K, Wu A. TLR9 expression in glioma tissues correlated to glioma progression and the prognosis of GBM patients. *BMC Cancer* 2010;10:415.
- Wang TR, Peng JC, Qiao YQ, Zhu MM, Zhao D, Shen J, Ran ZH. *Helicobacter pylori* regulates TLR4 and TLR9 during gastric carcinogenesis. *Int J Clin Exp Pathol* 2014; 7:6950–6955.

19. Dajon M, Iribarren K, Cremer I. Toll-like receptor stimulation in cancer: a pro- and anti-tumor double-edged sword. *Immunobiology* 2017;222:89–100.
20. Krieg AM. Development of TLR9 agonists for cancer therapy. *J Clin Invest* 2007;117:1184–1194.
21. Varga MG, Piazuelo MB, Romero-Gallo J, Delgado AG, Suarez G, Whitaker ME, Krishna US, Patel RV, Skaar EP, Wilson KT, Algood HM, Peek RM Jr. TLR9 activation suppresses inflammation in response to *Helicobacter pylori* infection. *Am J Physiol Gastrointest Liver Physiol* 2016;311:G852–G858.
22. Otani K, Tanigawa T, Watanabe T, Nadatani Y, Sogawa M, Yamagami H, Shiba M, Watanabe K, Tominaga K, Fujiwara Y, Arakawa T. Toll-like receptor 9 signaling has anti-inflammatory effects on the early phase of *Helicobacter pylori*-induced gastritis. *Biochem Biophys Res Commun* 2012;426:342–349.
23. Anderson AE, Worku ML, Khamri W, Bamford KB, Walker MM, Thursz MR. TLR9 polymorphisms determine murine lymphocyte responses to *Helicobacter*: results from a genome-wide scan. *Eur J Immunol* 2007;37:1548–1561.
24. Ooi C, Ivanova T, Wu J, Lee M, Tan IB, Tao J, Ward L, Koo JH, Gopalakrishnan V, Zhu Y, Cheng LL, Lee J, Rha SY, Chung HC, Ganesan K, So J, Soo KC, Lim D, Chan WH, Wong WK, Bowtell D, Yeoh KG, Grabsch H, Boussioutas A, Tan P. Oncogenic pathway combinations predict clinical prognosis in gastric cancer. *pLoS Genet* 2009;5:e1000676.
25. Balic JJ, Garama DJ, Saad MI, Yu L, West AC, West AJ, Livis T, Bhathal PS, Gough DJ, Jenkins BJ. Serine-phosphorylated STAT3 promotes tumorigenesis via modulation of RNA polymerase transcriptional activity. *Cancer Res* 2019;79:5272–5287.
26. Jenkins BJ, Graill D, Nheu T, Najdovska M, Wang B, Waring P, Inglese M, McLoughlin RM, Jones SA, Topley N, Baumann H, Judd LM, Giraud AS, Boussioutas A, Zhu HJ, Ernst M. Hyperactivation of Stat3 in gp130 mutant mice promotes gastric hyperproliferation and desensitizes TGF-beta signaling. *Nat Med* 2005;11:845–852.
27. Poh AR, Dwyer AR, Eissmann MF, Chand AL, Baloyan D, Boon L, Murrey MW, Whitehead L, Brien M, Lowell CA, Putoczki TL, Pixley FJ, Donoghue RJJ, Ernst M. Inhibition of the SRC kinase HCK impairs STAT3-dependent gastric tumor growth in mice. *Cancer Immunol Res* 2020;8:428–435.
28. Lee A, Fox JG, Otto G, Murphy J. A small animal model of human *Helicobacter pylori* active chronic gastritis. *Gastroenterology* 1990;99:1315–1323.
29. Sigal M, Rothenberg ME, Logan CY, Lee JY, Honaker RW, Cooper RL, Passarelli B, Camorlinga M, Bouley DM, Alvarez G, Nusse R, Torres J, Amieva MR. *Helicobacter pylori* activates and expands Lgr5(+) stem cells through direct colonization of the gastric glands. *Gastroenterology* 2015;148:1392–1404 e21.
30. Lennerz JK, Kim SH, Oates EL, Huh WJ, Doherty JM, Tian X, Bredemeyer AJ, Goldenring JR, Lauwers GY, Shin YK, Mills JC. The transcription factor MIST1 is a novel human gastric chief cell marker whose expression is lost in metaplasia, dysplasia, and carcinoma. *Am J Pathol* 2010;177:1514–1533.
31. Choi E, Hendley AM, Bailey JM, Leach SD, Goldenring JR. Expression of activated Ras in gastric chief cells of mice leads to the full spectrum of metaplastic lineage transitions. *Gastroenterology* 2016;150:918–930 e13.
32. Min J, Vega PN, Engevik AC, Williams JA, Yang Q, Patterson LM, Simmons AJ, Bliton RJ, Betts JW, Lau KS, Magness ST, Goldenring JR, Choi E. Heterogeneity and dynamics of active Kras-induced dysplastic lineages from mouse corpus stomach. *Nat Commun* 2019;10:5549.
33. Tsugawa H, Kato C, Mori H, Matsuzaki J, Kameyama K, Saya H, Hatakeyama M, Suematsu M, Suzuki H. Cancer stem-cell marker CD44v9-positive cells arise from *Helicobacter pylori*-infected CAPZA1-overexpressing cells. *Cell Mol Gastroenterol Hepatol* 2019;8:319–334.
34. Eaton KA, Mefford M. Cure of *Helicobacter pylori* infection and resolution of gastritis by adoptive transfer of splenocytes in mice. *Infect Immun* 2001;69:1025–1031.
35. Li JK, Balic JJ, Yu L, Jenkins BJ. TLR agonists as adjuvants for cancer vaccines. *Adv Exp Med Biol* 2017;1024:195–212.
36. Kim IY, Yan X, Tohme S, Ahmed A, Cordon-Cardo C, Shantha Kumara HM, Kim SK, Whelan RL. CpG ODN, toll like receptor (TLR)-9 agonist, inhibits metastatic colon adenocarcinoma in a murine hepatic tumor model. *J Surg Res* 2012;174:284–290.
37. El Andaloussi A, Sonabend AM, Han Y, Lesniak MS. Stimulation of TLR9 with CpG ODN enhances apoptosis of glioma and prolongs the survival of mice with experimental brain tumors. *Glia* 2006;54:526–535.
38. Herrmann A, Cherryholmes G, Schroeder A, Phallen J, Alizadeh D, Xin H, Wang T, Lee H, Lahtz C, Swiderski P, Armstrong B, Kowolik C, Gallia GL, Lim M, Brown C, Badie B, Forman S, Kortylewski M, Jove R, Yu H. TLR9 is critical for glioma stem cell maintenance and targeting. *Cancer Res* 2014;74:5218–5228.
39. Rad R, Ballhorn W, Volland P, Eisenacher K, Mages J, Rad L, Ferstl R, Lang R, Wagner H, Schmid RM, Bauer S, Prinz C, Kirschning CJ, Krug A. Extracellular and intracellular pattern recognition receptors cooperate in the recognition of *Helicobacter pylori*. *Gastroenterology* 2009;136:2247–2257.
40. Alvarez-Arellano L, Cortés-Reynosa P, Sánchez-Zauco N, Salazar E, Torres J, Maldonado-Bernal C. TLR9 and NF- $\kappa$ B are partially involved in activation of human neutrophils by *Helicobacter pylori* and its purified DNA. *pLoS One* 2014;9:e101342.
41. Ishii Y, Shibata W, Sugimori M, Kaneta Y, Kanno M, Sato T, Sue S, Kameta E, Kaneko H, Irie K, Sasaki T, Kondo M, Maeda S. Activation of signal transduction and activator of transcription 3 signaling contributes to *Helicobacter*-associated gastric epithelial proliferation and inflammation. *Gastroenterol Res Pract* 2018;2018:9050715.
42. Sokolova O, Naumann M. NF- $\kappa$ B signaling in gastric cancer. *Toxins (Basel)* 2017;9:119.
43. Ying L, Ferrero RL. Role of NOD1 and ALPK1/TIFA signalling in innate immunity against *Helicobacter pylori*

- infection. *Curr Top Microbiol Immunol* 2019; 421:159–177.
44. Ng MT, Va't Hof R, Crockett JC, Hope ME, Berry S, Thomson J, McLean MH, McColl KE, El-Omar EM, Hold GL. Increase in NF-kappaB binding affinity of the variant C allele of the toll-like receptor 9 -1237T/C polymorphism is associated with Helicobacter pylori-induced gastric disease. *Infect Immun* 2010; 78:1345–1352.
  45. Algood HM, Gallo-Romero J, Wilson KT, Peek RM Jr, Cover TL. Host response to Helicobacter pylori infection before initiation of the adaptive immune response. *FEMS Immunol Med Microbiol* 2007;51:577–586.
  46. Kaparakis M, Walduck AK, Price JD, Pedersen JS, Van Rooijen N, Pearse MJ, Wijburg OL, Strugnell RA. Macrophages are mediators of gastritis in acute Helicobacter pylori infection in C57BL/6 mice. *Infect Immun* 2008; 76:2235–2239.
  47. Quiding-Jarbrink M, Raghavan S, Sundquist M. Enhanced M1 macrophage polarization in human helicobacter pylori-associated atrophic gastritis and in vaccinated mice. *pLoS One* 2010;5:e15018.
  48. Lehours P, Ferrero RL. Review: Helicobacter— inflammation, immunology, and vaccines. *Helicobacter* 2019;24(Suppl 1):e12644.
  49. Kennedy CL, Najdovska M, Jones GW, McLeod L, Hughes NR, Allison C, Ooi CH, Tan P, Ferrero RL, Jones SA, Dev A, Sievert W, Bhathal PS, Jenkins BJ. The molecular pathogenesis of STAT3-driven gastric tumorigenesis in mice is independent of IL-17. *J Pathol* 2011;225:255–264.
  50. Ernst M, Najdovska M, Grail D, Lundgren-May T, Buchert M, Tye H, Matthews VB, Armes J, Bhathal PS, Hughes NR, Marcusson EG, Karras JG, Na S, Sedgwick JD, Hertzog PJ, Jenkins BJ. STAT3 and STAT1 mediate IL-11-dependent and inflammation-associated gastric tumorigenesis in gp130 receptor mutant mice. *J Clin Invest* 2008;118:1727–1738.
  51. Hemmi H, Takeuchi O, Kawai T, Kaisho T, Sato S, Sanjo H, Matsumoto M, Hoshino K, Wagner H, Takeda K, Akira S. A toll-like receptor recognizes bacterial DNA. *Nature* 2000;408:740–745.
  52. Chonwerawong M, Ferrand J, Chaudhry HM, Higgins C, Tran LS, Lim SS, Walker MM, Bhathal PS, Dev A, Moore GT, Sievert W, Jenkins BJ, Elios MM, Philpott DJ, Kufer TA, Ferrero RL. Innate immune molecule NLRC5 protects mice from Helicobacter-induced formation of gastric lymphoid tissue. *Gastroenterology* 2020; 159:169–182 e8.
  53. Ferrero RL, Wilson JE, Sutton P. Mouse models of Helicobacter-induced gastric cancer: use of co-carcinogens. *Methods Mol Biol* 2012;921:157–173.
  54. Balic JJ, Saad MI, Dawson R, West AJ, McLeod L, West AC, Costa K, Deswaerte V, Dev A, Sievert W, Gough DJ, Bhathal PS, Ferrero RL, Jenkins BJ. Constitutive STAT3 serine phosphorylation promotes Helicobacter-mediated gastric disease. *Am J Pathol* 2020;190:1256–1270.
  55. Velin D, Favre L, Bernasconi E, Bachmann D, Pythoud C, Saiji E, Bouzourene H, Michetti P. Interleukin-17 is a critical mediator of vaccine-induced reduction of Helicobacter infection in the mouse model. *Gastroenterology* 2009;136:2237–2246.
  56. Schneider CA, Rasband WS, Eliceiri KW. NIH Image to ImageJ: 25 years of image analysis. *Nat Methods* 2012; 9:671–675.
  57. Dawson RE, Deswaerte V, West AC, Tang K, West AJ, Balic JJ, Gearing LJ, Saad MI, Yu L, Wu Y, Bhathal PS, Kumar B, Chakrabarti JT, Zavros Y, Oshima H, Klinman DM, Oshima M, Tan P, Jenkins BJ. STAT3-mediated upregulation of the AIM2 DNA sensor links innate immunity with cell migration to promote epithelial tumorigenesis. *Gut* 2021. <https://doi.org/10.1136/gutjnl-2020-323916>.
  58. Deswaerte V, Nguyen P, West A, Browning AF, Yu L, Ruwanpura SM, Balic J, Livis T, Girard C, Preaudet A, Oshima H, Fung KY, Tye H, Najdovska M, Ernst M, Oshima M, Gabay C, Putoczki T, Jenkins BJ. Inflammasome adaptor ASC suppresses apoptosis of gastric cancer cells by an IL18-mediated inflammation-independent mechanism. *Cancer Res* 2018;78:1293–1307.

---

Received February 7, 2021. Accepted June 6, 2022.

#### Correspondence

Address correspondence to: Brendan J. Jenkins, PhD, Centre for Innate Immunity and Infectious Diseases, Hudson Institute of Medical Research, 27-31 Wright Street, Clayton, Victoria 3168, Australia. e-mail: [Brendan.Jenkins@hudson.org.au](mailto:Brendan.Jenkins@hudson.org.au).

#### CRedit Authorship Contributions

Ke Tang (Formal analysis: Supporting; Investigation: Lead; Methodology: Lead)  
 Louise McLeod (Data curation: Equal)  
 Thaleia Livis (Formal analysis: Supporting; Investigation: Supporting; Methodology: Supporting)  
 Alison West (Formal analysis: Supporting; Investigation: Supporting; Methodology: Supporting)  
 Ruby Dawson (Data curation: Equal)  
 Liang Yu (Investigation: Supporting; Methodology: Supporting)  
 Jesse Balic (Investigation: Supporting; Methodology: Supporting)  
 Michelle Chonwerawong (Investigation: Supporting; Methodology: Supporting)  
 Georgie Wray-mccann (Investigation: Supporting; Methodology: Supporting)  
 Hiroko Oshima (Data curation: Equal)  
 Masanobu Oshima (Data curation: Equal)  
 Virginie Deswaerte (Investigation: Supporting; Methodology: Supporting)  
 Richard Ferrero (Funding acquisition: Supporting; Methodology: Supporting; Resources: Supporting; Supervision: Supporting; Writing – review & editing: Supporting)  
 Brendan Jenkins (Conceptualization: Lead; Data curation: Lead; Formal analysis: Lead; Funding acquisition: Lead; Project administration: Lead; Resources: Lead; Supervision: Lead; Validation: Lead; Writing – original draft: Lead)

#### Conflicts of interest

The authors disclose no conflicts.

#### Funding

Supported by research grants from the National Health and Medical Research Council (NHMRC) of Australia awarded to B.J. Jenkins (APP1139371) and R. L. Ferrero (APP1107930), as well as the Operational Infrastructure Support Program by the Victorian Government of Australia. K. Tang was supported by Monash Graduate and Monash International Postgraduate Research Scholarships. R.L. Ferrero (APP1079904) and B.J. Jenkins (APP1154279) are supported by NHMRC Senior Research Fellowships.